Supporting Information

SI Methods

EWS-FLI1 interacting partners identified through MS. We developed an unbiased screen for potential partners that interact with EWS-FLI1 by adding ES nuclear lysate to immobilized EWS-FLI1, followed by elution and PAGE. Nuclear lysate from Ewing sarcoma (ES) cell line TC32 was added to two Hi-TRAP Ni charged columns in series, with only the second column containing EWS-FLI1. Following the addition of nuclear lysate and wash, the columns were separated and independently eluted with imidazole. Fractions were resolved on both high (14%) and low (6%) polyacrylamide gels, followed by Coomassie staining and protein bands of interest were manually excised and subjected to in-gel tryptic digestion. Protein digests separation was performed on an Aquity UPLC BEH 130 C18 column and followed by mass spectrometry (MS). Mass spectra were acquired online using a nano-ESI-LC-MS/MS QStar Elite (ABSCIEX) and operated with Analyst QS v2.0 data acquisition software. MS data were searched against the SWISS-PROT databases using ProteinPilot software 3.0 and Paragon Algorithm to identify the individual proteins. Positive identification of proteins eluting with EWS-FLI1 was rigorous including: (i) band from the gel located near estimated molecular weight, (ii) greater than 95% ion confidence interval, and (iii) 99% confidence in peptide assignment based upon greater than 3 peptides. Proteins eluted from a Ni-charged column without EWS-FLI1 were considered non-specific. Proteins were identified in three separate experiments starting from EWS-FLI1 and fresh nuclear lysate to insure reproducibility.

Nuclear Co-Immunoprecipitation. Co-Immunoprecipitation (Co-IP) was used to pull down protein partners of a protein of interest using an antibody that specifically binds to this specific protein in order to test protein-protein interaction. Active motif universal magnetic Co-IP kit (Active Motif) was used to make nuclear extract from TC32 cells. The protein G magnetic beads were used for Co-IP and the IP was performed on 300 μg samples using 2 μg of FLI1/PRPF8/DDX5 polyclonal antibody and rabbit IgG (as a negative control). Western blot was then performed individually using the following antibodies FLI1 (Santa Cruz Biotechnology, USA), DDX5, PRPF6, hnRNP K, RHA, hnRNP U, CDC5L, DDX17, SF3B3, SF3B2, SF3A2, PRPF8, SFPQ (Abcam, USA) and snRNP200 (Sigma-Aldrich, USA), on 10 μg input nuclear extract, FLI1/PRPF8/DDX5 IP and the rabbit IgG IP.

ELISA. ELISA was performed on maxi sorb 96 well plate. Recombinant full length EWS-FLI1 protein (300 ng) were coated on the bottom surface of the ELISA plate overnight and followed by blocked with 4% BSA. Spliceosomal proteins DDX5, PRPF6, hnRNP K, RHA, hnRNP U, CDC5L, DDX17, SF3B3 and SF3B2 were used as ligand to detect the specific protein interaction using anti-DDK monoclonal antibody with HRP conjugated (for RHA protein goat anti-RHA antibody (Everest)), protein binding was detected using 3,3',5,5'-tetramethylbenzidine (TMB) peroxidase substrate kit (Bio-Rad, CA) per the manufacturer's instructions. The substrate reaction is incubated at room temperature with periodic mixing (e.g., 2-3 seconds shaking in the plate reader) and the color development monitored by absorbance reading at 415 nm or 405 nm using a microplate reader. Negative controls for each ELISA included the absence of EWS-FLI1, absence of second recombinant protein, and blocking alone were used. For the positive control, ELISA plate wells were coated with their corresponding spliceosomal proteins and their corresponding secondary antibody.

Method for drawing networks. The proteins identified by MS as a potential interactive partner of EWS-FLI1 are included and followed by proteomic analysis were used as input for Ingenuity Pathway Analysis to identify networks of interacting proteins. Using IPA, clusters of proteins appearing in the top functional pathways and networks with the most highly significant p-values were selected for constructing the network. IPA uses a curated proprietary knowledgebase to identify protein interactions based on experimental evidence gathered from published reports. The resulting networks thus generated were filtered for direct and indirect interactions, and trimmed to remove nodes beyond the second level of interactions from the proteins of interest. Direct binding partners that appeared within this network were confirmed by experimental validations.

Affymetrix Exon Array. Total RNA was extracted using Qiagen AllPrep DNA/RNA/Protein kit from each of the derived cell lines (9 cell lines with/without EWS-FLI1). The RNA quality was measured using Agilent 2100 bioanalyzer and RNA Integrity number (RIN) above 9.60 were used for Exon array experiments. cDNA was synthesized and hybridized to Affymetrix GeneChip Human Exon 1.0 ST microarray chips and .CEL files are generated. These raw data files were processed using two analytical tools, PGS and easyExon. All data CEL files were uploaded to GEO and their Accession number is GSE65941.

Data preparation and analysis for PGS. Data was pre-processed using Partek Genomic Suite software (PGS v6.6, Partek Inc., St. Louis, MO) with the Affymetrix-annotated core probe set. The configuration consisted of a pre-background adjustment for GC content and probe sequence, Robust Multi-array Analysis (RMA) (1) for background correction, quantile normalization and probe set summarization using median polish. All signals were log2-transformed. Library files were those specified by Affymetrix (hg18). Differential expression was determined by ANOVA. The multiple test correction implemented the p-value method to determine a false discovery rate (FDR) < 0.05. Exon level data was filtered using Detection Above Background (DABG; (2)). Data was analyzed for alternative splicing by a repeated measure AS-ANOVA. The p-value method was used to control the FDR with a cutoff <0.05 to determine the presence of alternative exon usage.

Data analysis for easyExon. easyExon uses RMA for background correction and probe set summarization. Microarray detection of alternative splicing (MIDAS) p-value <0.05 and pattern-based correlation (PAC) are used to determine significant AS transcripts (3). The degree of AS was visualized by the spicing index (SI) plot. In addition, the intensity fold change $> \pm 2$ was also calculated to show the differentially expressed genes.

Exon array validation by Quantitative real-time polymerase chain reaction (qRT-PCR). Exon array findings (both expression and alternative splicing) were validated using qRT-PCR on the several genes focused on in this study. Validation of alternative splicing was performed using 2 different primer-pair combinations within the same transcript (RefSeq - release 61). One pair of primers target an area that can be used to differentiate between isoforms, and a second pair target an area common to all transcripts of the gene. The latter was used to normalize endogenous expression. Transcript expression validation used 18S as the internal normalizer gene with the primer set for the transcript of interest.

RNAseq analysis and MISO. 100 million paired-end reads were aligned to hg19 using TopHat2/Bowtie2 (4, 5) with default parameters for genome-guided transcriptome reconstruction. MISO version 0.5.2 was used to estimate PSI values (6). Version 2 reference annotation includes annotated splicing events found in Ensembl genes, UCSC knownGenes, and RefSeq genes. Version 2 includes annotation of skipped exons, retained introns, mutually exclusive exons, and alternative 5'/3' splice sites. Discovered splicing events were filtered for those with a PSI difference greater than 20% as well as a Bayes factor greater than 10. Probability of overlap between sets of splicing events found in either shEWS-FLI1 or YK-4-279 was calculated using a hypergeometric distribution specific to the total number of annotated events of each type.

RNA immunoprecipitation (RIP) and Cross-linked RNA immunoprecipitation (CLIP). RIP was carried out as previously published (7). CLIP was carried out using FLI1 antibody from Innovagen (Sweden) raised against recombinant FLI1 C- terminal protein in rabbit. TC32 cells were UV crosslinked at 150 mJ/cm^2 in Stratalinker (Invitrogen). The CLIP protocol was followed as published previously (8).

CLIPseq analysis and MEME suite. CLIPseq reads were trimmed for barcode and CLIP adapter sequences and PCR duplicated were removed. Filtered reads were then aligned to hg19 using Bowtie version 1.1.1 (9, 10). Those reads that aligned unambiguously were used in downstream processing. Sequence of forward and reverse reads were treated separately as MEME inputs (11). The top motif with a corresponding reverse complement motif in the reverse set was considered as the lead motif for further analysis.

Motif localization and secondary structure MFE prediction. All higher-level data analysis was done in R using Bioconductor packages or at the UNIX command line (12, 13). The *BSgenome* and *GenomicRanges* R packages were used to extract genomic sequence +/-125bp of the 5' and 3' ends of all exons annotated in hg19. These sets were searched for occurrences of the lead motif with ≥ 90% match to the motif position weight matrix. Frequency of hits were graphed with respect to the exon-intron boundary for the 5' and 3' sets separately. Local secondary structure prediction was performed using RNALFold version 2.1.8. Local secondary structure was defined as 200nt or less, not including g-quadruplex formation. Minimum free energy for each read sequenced and aligned greater than 20nt long was recorded. A null set was generated by taking random exonic sequences of the same length as each CLIP read. These two minimum free energy density profiles were plotted together to compare local secondary structure preference of EWS-FLI1 RNA binding.

Minigene cloning and transfection. TERT minigene was synthesized using the three exons and two introns (300 bp on the either side of exon-intron junction) and subcloned them into pcDNA3.1+ vector (GenScript). We transfected a total of 6 μg of minigene plasmid into 50% confluent TC32 cells using X-treme Gene 9 DNA transfection reagent (Roche Diagnostics) (14).

γ-TERT Construct and Telomeric Repeat Amplification Protocol (TRAP) assay. pBABE-puro-hTERT plasmid was a gift from Dr. Elizabeth Blackburn (UCSF) (15). We designed a pair of exon11 deletion primer as Forward: CTATGCCCGGACCTCCAT; Reverse: CTGAGGAAGGTTTTCGCG. When PCR is conducted to amplify hTERT, this primer allow to skip full length of E11(189bp, 36767-36925, genbank ID NM_198253.2). Exon 11 deleted

pBABE-puro-hTERT-E11null plasmid was constructed Using Q5 Site-Directed Mutagenesis Kit (NEB, MA,USA). Briefly, hTERT PCR amplification was done with above primer and mastermix from the kit, according to the cycling condition provided by NEB. Template DNA were eliminated and product DNA were ligated by KLD buffer provided by NEB (kinase, ligase and DpnI enzymes). The deletion of exon 11 (γ-TERT) was verified by sequencing. Real time quantitative TRAP for detection of telomerase activity was performed (16).

BruDRB-seq. The labeling of nascent RNA with bromouridine (Bru) was carried out as described (17). For BruDRB-seq, the drug 5,6- dichlorobenzimidazole 1-b-D-ribofuranoside (Sigma) was used and the details are as described (18). Finally, cDNA libraries were made from the Bru-labeled RNA using the Illumina TruSeq library kit and sequenced using Illumina HiSeq sequencers at the University of Michigan DNA Sequencing Core. The sequencing and read mapping were carried out as described (17).

Clinical Information. The EE99 trial employed VIDE induction chemotherapy (6 cycles of vincristine, ifosfamide, doxorubicin and etoposide given approximately every 3 weeks prior to local control), followed by risk adapted randomized treatment (19). The EICESS-92 trial investigated whether cyclophosphamide could be used instead of ifosfamide in consolidation chemotherapy of standard-risk Ewing sarcoma (<100mL localized tumors). Standard risk patients with localized disease and a small tumor volume of < 100 ml were randomized for eight courses of consolidation chemotherapy with either ifosfamide (VAIA) or cyclophosphamide (VACA). High risk patients with large tumor volume and /or metastases were randomized for VAIA or EVAIA (20).

Analysis of human tumor exon data and splicing evaluation. In a previous study, human tumor samples were hybridized to Affymetrix Human Exon 1.0 ST v2 arrays and their data CEL files were already deposited in GEO (GSE63157). For the NC data CEL files GEO Accession number GSE21511. MDA-MB-231 exon array data CEL files were downloaded from GEO Accession number GSE47013. Probeset-level and gene-level intensities were normalized using RMA from the Bioconductor package "oligo" (12, 21, 22). The quality of each array was assessed using arrayQualityMetrics (23). Batch effects were corrected using ComBat (24). We calculated gene-normalized exon expressions by normalizing each probeset expression level with the associated meta-probeset, or gene-level expression, as annotated in the Affymetrix chip definition file. We used the Affymetrix set of core probes to estimate gene-level expression for downstream analysis and exon normalization. In this way, gene-normalized exon expressions were generated for each of the probesets for all genes in the core chip definition file. All computational analysis was done in R using Bioconductor.

Analysis/statistics for exon array comparisons. Plots comparing gene-normalized exon expressions were generated by retrieving all of the probesets associated with our 10 genes of interest and plotting each of their respective mean values by sample subset. Graphs mapping each of these sets were generated using the GenomeGraphs package (25). Pearson's *r* was used to assess the similarity of ESTS and TC32 control normalized exon-expression graphs. The location of the probeset used for detailed analysis is marked with an open arrow on the full probeset expression map. All gene-normalized exon expressions were centered and scaled for PCA analysis. Hierarchical cluster analysis used Ward's minimum variance for separation of Euclidean distances within the first three principal components.

1. Dyson HJ & Wright PE (2005) Intrinsically unstructured proteins and their functions. *Nat Rev Mol Cell Biol* 6(3):197-208.
2. Dunker AK & Obradovic Z (2001) The protein trinity--linking function and disorder. *Nat Biotechnol* 19(9):805-806.
3. Chang TY, *et al.* (2008) easyExon--a Java-based GUI tool for processing and visualization of Affymetrix exon array data. *BMC Bioinformatics* 9:432.
4. Kim D, *et al.* (2013) TopHat2: accurate alignment of transcriptomes in the presence of insertions, deletions and gene fusions. *Genome Biol* 14(4):R36.
5. Langmead B & Salzberg SL (2012) Fast gapped-read alignment with Bowtie 2. *Nat Methods* 9(4):357-359.
6. Katz Y, Wang ET, Airoldi EM, & Burge CB (2010) Analysis and design of RNA sequencing experiments for identifying isoform regulation. *Nat Methods* 7(12):1009-1015.
7. Erkizan HV, *et al.* (2015) RNA helicase A activity is inhibited by oncogenic transcription factor EWS-FLI1. *Nucleic Acids Res*.
8. Darnell R (2012) CLIP (cross-linking and immunoprecipitation) identification of RNAs bound by a specific protein. *Cold Spring Harbor protocols* 2012(11):1146-1160.
9. Trapnell C, Pachter L, & Salzberg SL (2009) TopHat: discovering splice junctions with RNA-Seq. *Bioinformatics* 25(9):1105-1111.
10. Kim D & Salzberg SL (2011) TopHat-Fusion: an algorithm for discovery of novel fusion transcripts. *Genome Biol* 12(8):R72.
11. Bailey TL & Elkan C (1994) Fitting a mixture model by expectation maximization to discover motifs in biopolymers. *Proceedings / ... International Conference on Intelligent Systems for Molecular Biology ; ISMB. International Conference on Intelligent Systems for Molecular Biology* 2:28-36.
12. Gentleman RC, *et al.* (2004) Bioconductor: open software development for computational biology and bioinformatics. *Genome Biol* 5(10):R80.
13. Ihaka R & Gentleman R (1996) R: a language for data analysis and graphics. *Journal of computational and graphical statistics* 5.3:299-314.
14. Roca X, *et al.* (2012) Widespread recognition of 5' splice sites by noncanonical base-pairing to U1 snRNA involving bulged nucleotides. *Genes Dev* 26(10):1098-1109.
15. Kim M, Xu L, & Blackburn EH (2003) Catalytically active human telomerase mutants with allele-specific biological properties. *Exp Cell Res* 288(2):277-287.
16. Stoppler H, Hartmann DP, Sherman L, & Schlegel R (1997) The human papillomavirus type 16 E6 and E7 oncoproteins dissociate cellular telomerase activity from the maintenance of telomere length. *J Biol Chem* 272(20):13332-13337.
17. Paulsen MT, *et al.* (2014) Use of Bru-Seq and BruChase-Seq for genome-wide assessment of the synthesis and stability of RNA. *Methods* 67(1):45-54.
18. Veloso A, *et al.* (2014) Rate of elongation by RNA polymerase II is associated with specific gene features and epigenetic modifications. *Genome Res* 24(6):896-905.
19. Ladenstein R, *et al.* (2010) Primary disseminated multifocal Ewing sarcoma: results of the Euro-EWING 99 trial. *J Clin Oncol* 28(20):3284-3291.

20. Schuck A*, et al.* (2003) Local therapy in localized Ewing tumors: results of 1058 patients treated in the CESS 81, CESS 86, and EICESS 92 trials. *Int J Radiat Oncol Biol Phys* 55(1):168-177.
21. Irizarry RA*, et al.* (2003) Exploration, normalization, and summaries of high density oligonucleotide array probe level data. *Biostatistics* 4(2):249-264.
22. Carvalho BS & Irizarry RA (2010) A framework for oligonucleotide microarray preprocessing. *Bioinformatics* 26(19):2363-2367.
23. Kauffmann A, Gentleman R, & Huber W (2009) arrayQualityMetrics--a bioconductor package for quality assessment of microarray data. *Bioinformatics* 25(3):415-416.
24. Johnson WE, Li C, & Rabinovic A (2007) Adjusting batch effects in microarray expression data using empirical Bayes methods. *Biostatistics* 8(1):118-127.
25. Durinck S, Bullard J, Spellman PT, & Dudoit S (2009) GenomeGraphs: integrated genomic data visualization with R. *BMC Bioinformatics* 10:2.

Primers used for qRT-PCR

Primer #	Gene Name	Forward (5'-3')	Reverse (5'-3')
600	ARID1A	AATCAGTTCTCCACCCAAGG	GTACATCTCCCCTTCGTGC
601	ARID1A	GCGGCTCACAATGAAAGAC	AGGAGACCAGACTTGAGGG
602	ARID1A	AGCAACGACATGATTCCTATGG	AGGTGCGGTTCTCCATTG
604	EZH2	CCTGACCTCTGTCTTACTTGTG	AGATGGTGCCAGCAATAGATG
605	EZH2	GACTTCTGTGAGCTCATTGC	CATTATGGGTACTGAAGCAACTG
605A	EZH2	TCGGTCCGGTCGCGTCCGACA	GAGCTGTCTCAGTCGCATGT
606	EZH2	TGCTTCCTACATCGTAAGTGC	CAAATGCTGGTAACACTGTGG
607A	EZH2	TGACAGTTCGTGCCCTTG	AGATGGTGCCAGCAATAGATG
607B	EZH2	GACTTCTGTGAGCTCATTGC	TCCTGATCTAAAACTTCATCTCCC
607C	EZH2	CGTCCTGTTGAATTCCCACT	TGGCCCATGATTATTTAGGC
608	MBNL1	AGCAAATGCAACTAGCCAATG	CCAGATAGGGATTAAAGGCGG
609	MBNL1	AGATGCTCTCGGGAAAAGTG	AGTGATTTGACAGCCGACTG
610	MBNL1	GCTGTCAAATCACTGAAGCG	AGTGTTAAAGACTGCGGTGG
611	MBNL1	ATACAGCATTTCTCCCACCAG	GCTAGTCAGATGTTCGGCAG
612	MBNL1	ACAAGTGTTCCCTTCGCTG	ACTGTCCTTTCCTCTTTAGCATG
613	MBNL1	GCACATCCTTCGAAAAGCTG	TGCGTCCATTTATCTCCAACTG
614	MBNL1	TGTTGGTTACAGGGAATCCG	GCAAACCGACAATCATTTTCTCC
614A	MBNL1	GCTGTCAAATCACTGAAGCG	GCTAGTCAGATGTTCGGCAG
614B	MBNL1	AGCAAATGCAACTAGCCAATG	GCAAACCGACAATCATTTTCTCC
615	CUL4A	TGGTCATCAAGAACTTCCGAG	ATTTTCCACAGCCTGGTAGAG
615A	CUL4A	GCCAGCGGCTCTGATTAC	ACAGAGATTTTCCACAGCCTG
616	CUL4A	AGATTAACACGTGCTGGCAG	AACAGTTCTAATCCCATATCCCAG
617	BRF1	GCATCTCAGACTCCATCCG	GGGCTTCCGACTCATTCAG
618A	BRF1	GGTGCAGTTCGTGGAGAG	AGAAGTTGAAGGCGGTGTC
618B	BRF1	GTGTGGTACCCGAGAGAGGA	AGAAGTTGAAGGCGGTGTC
619	BRF1	ACCTTAGCATGCCCCGGTGTG	TGGGCTTGTGTTCCTTGTAG
620	BRF1	TTCAAGATGGCCGTGAGC	AGGACGGAGGCTGTCTACCT
621	BRF1	ATATGCAGGAAACCCCACAG	GTAACGACCACAGAGACACAG
622	BRF1	CCAAGACGTACTGGGAGGAG	TTGACCACACTGATGACCTCC
623	CAV3	AGACCCCAAGAACATTAACGAG	GTACTTGGAGACAGTGAAGGTG
624	CAV3	CTGCGGAAGGAGGTCTAAAG	GAGCAGTCCCTAAAGAGAAAGAG
624A	CAV3	CTGCGGAAGGAGGTCTAAAG	TACACCGTGTGCTCCATCAT
625	DACT3	TCTGGGACCTGGGACAG	CACAGAAGGTTGAGGGTGG
626	DACT3	ATGAGGATGAAGATGCGGC	TCCAGGCTCAGGTCTCC
627	DACT3	GGCCCAAGTCCCTAGGTAAG	TGTCACAGCTGGAATTGGAA
628	DACT3	CTCACTCAGACCCAT	CGCTCTCCTGTTCCAGGCC
629	DHX29	GAATGATTTCTGGAAGACTTACTGC	TCCAAGGCAGAATGAAGGTC
630	DHX29	AGCAAAGCAGGGGGAATAAA	AGATCCAGGTTGATTTTATGAGGA
632	TERT	AGAGTGTCTGGAGCAAGTTG	GATGAAGCGGAGTCTGGAC
633	TERT	TCTTCCTACGCTTCATGTGC	ACAGCTTGTTCTCCATGTCG
634A	TERT	GCACGGCTTTTGTTCAGATG	CTTGTAGATGTTGGTGCACAC
634P	TERT	ACGCGAAAACCTTCCTCAG	CGGTTGAAGGTGAGACTGG
640	USP2	GAGTTCAAGACCCAGATCCAG	GTTCTCAGGGTTGGACTTAGG
641	USP2	AGGATGTGCTTGATGGAGATG	CTTTGGGAACCTCTGGATGG
642	USP2	CGACTCGTCCATACTCCAAG	GCATAGTGGGCATCTGTGTAG
643A	USP2	CGACTCGTCCATACTCCAAG	GGCACTGCAGAATTGAGTTC

644	USP2	CACCTCGTACACCGTGACC	TTCTTGGCTTTGTTGAGCAG
645	CALD1	GGTTTCTAGCCGCATCAATG	TCCACAGATTGCTTTTCCCAG
646	CALD1	GTCACCAAGTCCTACCAGAAG	GCTTGCACTTTAGTTCCCTTC
647A	CALD1	GTCACCAAGTCCTACCAGAAG	AGGGCGGCTGAAAGTATTC
648	CALD1	TCTCCGTATCTCTCTGCCC	CCTCCTCTTCATCATCGTCATTC
649	CALD1	GGGTAGAATTTTGTTCAGTTTGG	TTGGAGCGATCCATTATCAG
650	CALD1	AGCTGTCCTAAAGAAACAGGG	TCTTCTTTGGGTTCTTTGTCCT
651	CALD1	TCTCCGTATCTCTCTGCCC	GCTTGCACTTTAGTTCCCTTC
652	CALD1	AGGGCGGTCTGGAGTTTTAT	CACCAATCCCTGTGGAATTT
654	CDKN1C	CAAGAGGCTGCGGTGAG	GCTACATGAACGGTCCCAG
655	CDKN1C	GGACGAGACAGGCGAAC	GCACTAGTACTGGGAAGGTC
656	CDKN1C	CTGACCAGCTGCACTCG	CTCAGGCGCTGATCTCTTG
657	CDKN1C	AGGCCAAGTGCGCTGTGCTCG	AGACGCTCCATCGTGGATGTG
658	CCND1	CATCTACACCGACAACTCCATC	TCTGGCATTTTGGAGAGGAAG
659	CCND1	CCTCGGTGTCCTACTTCAAATG	GCGGTCCAGGTAGTTCATG
660	CCND1	CCCGCACGATTTCATTGAAC	GGCGGATTGGAAATGAACTTC
661	CCND1	CCTCGGTGTCCTACTTCAAATG	GGCGGATTGGAAATGAACTTC
662	DCP2	AGGCTGGGGATTTCCAAAAG	GCAAGCTGGTCATTGATTCG
663	DCP2	TTATTTCCTGACGGTTCTCCTG	CTGTTTTCTGCCATTTCCCC
664	DCP2	CAGATTGAACTTGCCCATTGG	TTCCACATCTTCACCTTGAGG
665A	DCP2	ATCATGGAGACCAAACGGG	CAAAGACCTCTCTAGCAGCAC
666	DCP2	GGTGCAATTATTCTTGATGAGACAC	CAAAGACCTCTCTAGCAGCAC
667A	DCP2	TTATTTCCTGACGGTTCTCCTG	CCTGAAGTTTCCGTGGATGA
668	IGFBP3	CAGAGCACAGATACCCAGAAC	AGCACATTGAGGAACTTCAGG
669	IGFBP3	ACAACTGTGGCCATGACTGA	AGAGCTCTATGCAGCGTGTG
670	IGFBP3	TCCAGGTGAGCCGCCCGCGCCA	GGTGGAACTTGGGATCAGAC
672	RUNX1	TCGAAGTGGAAGAGGGAAAAG	TCATCTAGTTTCTGCCGATGTC
673A	RUNX1	TGTTTGCAGGGTCCTAACTC	TGGTAGGACTGATCGTAGGAC
674	RUNX1	AGGACGAATCACACTGAATGC	ACTGTGGGTACGAAGGAAATG
675	RUNX1	AAGTCTGAACCCAGCATAGTG	CCTCACCCCTCTAGCCCTAC
676	RUNX1	CTCCACTGCCTTTAACCCTC	TGACTTCTGCCTTAACATCTCC
677	RUNX2	TTCACCTTGACCATAACCGTC	GGCGGTCAGAGAACAAACTAG
678	RUNX2	GTTAATCTCCGCAGGTCACTAC	TGTTTGATGCCATAGTCCCTC
679	RUNX2	CCTCCTTGCCCCTCATTT	GCTCACGTCGCTCATTTTG
680	RUNX2	CATCACCGATGTGCCTAGG	TAAGTAAAGGTGGCTGGATAGTG
681	HDAC8	GGTTTTAAGCGGAAGATGGAG	CAAAGAATGCACCATACTGGC
682	HDAC8	AATTAACTGGTCTGGAGGGTG	TGCAGATCCAAATCCACGTAG
683	HDAC8	GTCCCGAGTATGTCAGTATGTG	TGGAGGTGAAACTGAATGCG
684	HDAC8	TGCTCCTTTAACATGACTCCAG	AAGTATGTCCAGCATCGAGC
685	HDAC8	GGTGACGTGTCTGATGTTGG	ATGCAAATGGGGAAGACAAG
686A	HDAC8	CGACGGAAATTTGAGCGTAT	ATGCAAATGGGGAAGACAAG
687	HDAC8	AGCATCTCCAGAAGGTCAGC	GGCCTAGGGAGGGTAATCAG
688	DIDO1	ACCGAAGCCTGAATGTGAG	AGCCTCAGAAATGCCCAC
689	DIDO1	CATCCAAACTCTTGCCCTTTG	GCTTTTCGTCCATCTTGTCTAAC
690	DIDO1	AGAGTCAAAAGGCGTCGG	GATTATCTAGAGGCTGTTCCCG
691	DIDO1	CGGAGCAAGAGCAAAGAGA	GTTCAACGCATCTTACGAACG
692	DIDO1	AAATGGCTGCGAGACCCTA	CAGGCTTCGTATTTTCAACAA
693	DIDO1	CATCCAAACTCTTGCCCTTTG	TCCTAACTCCTGCTCCCAG
694	DIDO1	GGAGTTGCAGCTTTGTGTTAAG	GCTTTGGAAAACAGTGACAGG
700	CLK1	ACCACAGTACTTCACATCGTC	CTACCTCCCGCTTTATGATCG

701	CASP3	TTGTGAGGCGGTTGTAGAAG	TCCAGAGTCCATTGATTCGC
707	PPFIBP1	AAAGTAACAAGAGAACAGCAAGTG	TGGAGGCGGTATCTGGAAG
900	TERT-MiniGene	GAGACCCAAGCTGGCTAGCGTT	GAGGCTGATCAGCGGGTTTAAAC

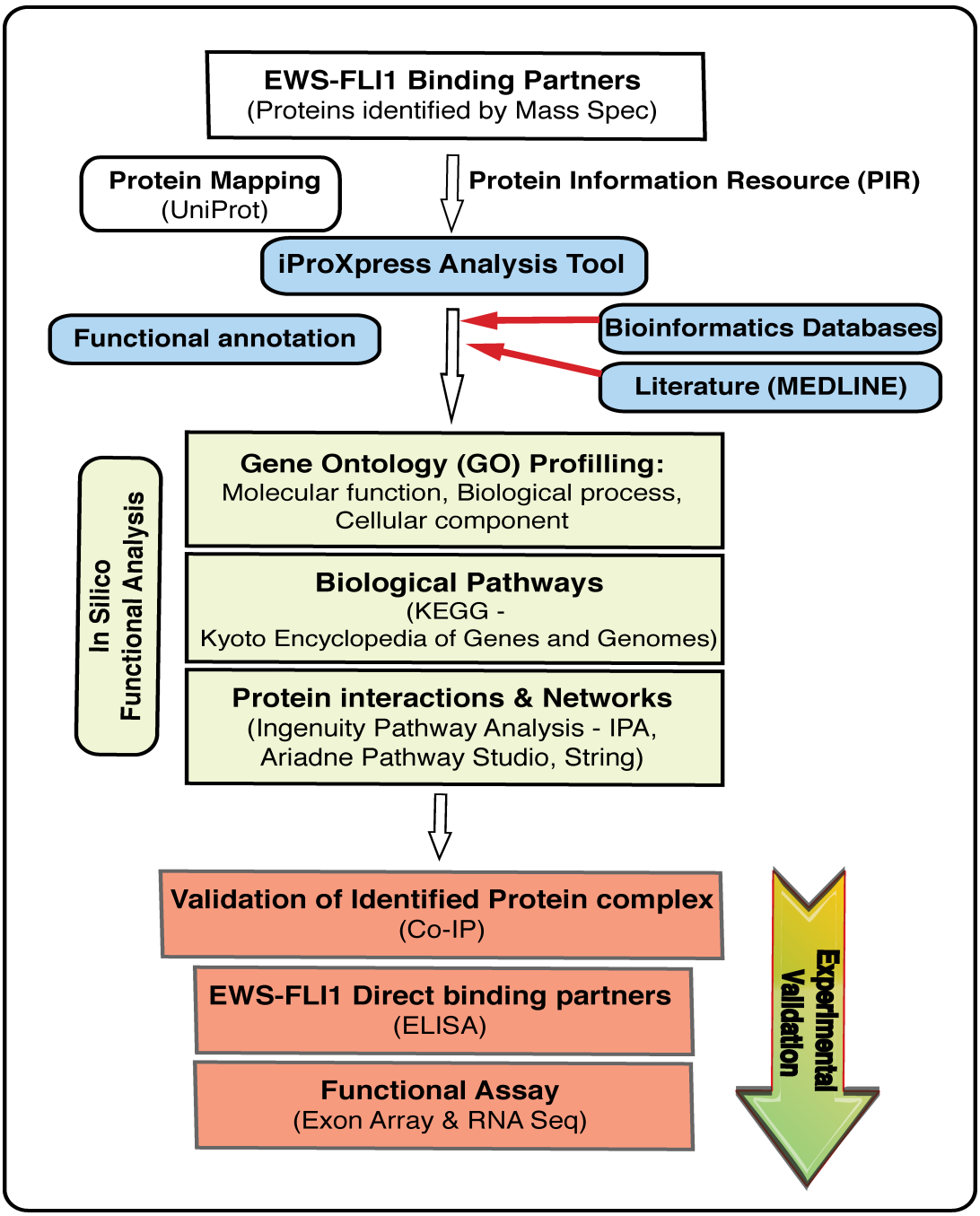

Fig. S1. Schema of EWS-FLI1 Partner Analysis. Functional annotations are derived for the list of proteins identified through MS as potential interactive partners of EWS-FLI1 are added in iProXpress analysis tool. Based on integrated data from multiple bioinformatics databases including text mining of literature and functional annotation, *in silico* functional analysis were carried out. Gene ontology (GO) profiling such as molecular function, biological process and cellular component. Biological pathways (KEGG) and protein interactions & networks using IPA, Ariadne pathway studio and String 9.0. Further, EWS-FLI1 interactive protein partners are confirmed by the following experimental validations including Co-IP and ELISA for indirect and direct protein partners. Exon array and RNA-seq were used to identify the functional aspects of the EWS-FLI1 and their association with spliceosomal complex.

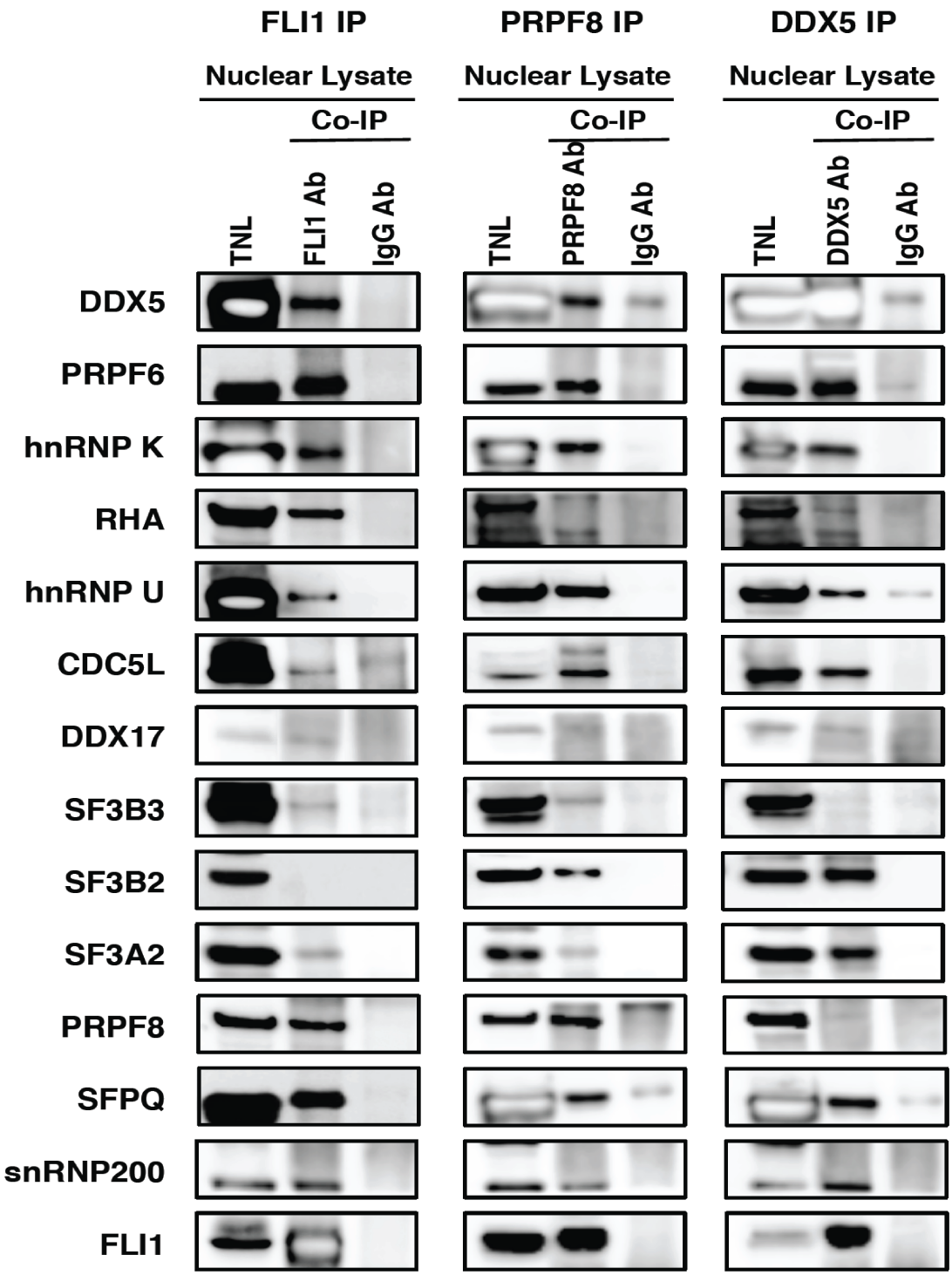

Fig. S2A. Experimental Validation of EWS-FLI1 Associated Spliceosomal Complex Proteins by Co-IP. Antibodies used for the co-IP are indicated on the top and antibodies used for the western blots are indicated on the left. 10% of total nuclear lysate (TNL) was used as input (lane 1), corresponding antibody pull downs showing the presence of proteins as a part of the complex (lane 2). For the negative control, rabbit polyclonal IgG antibody (Ab) was used to show specificity (lane 3).

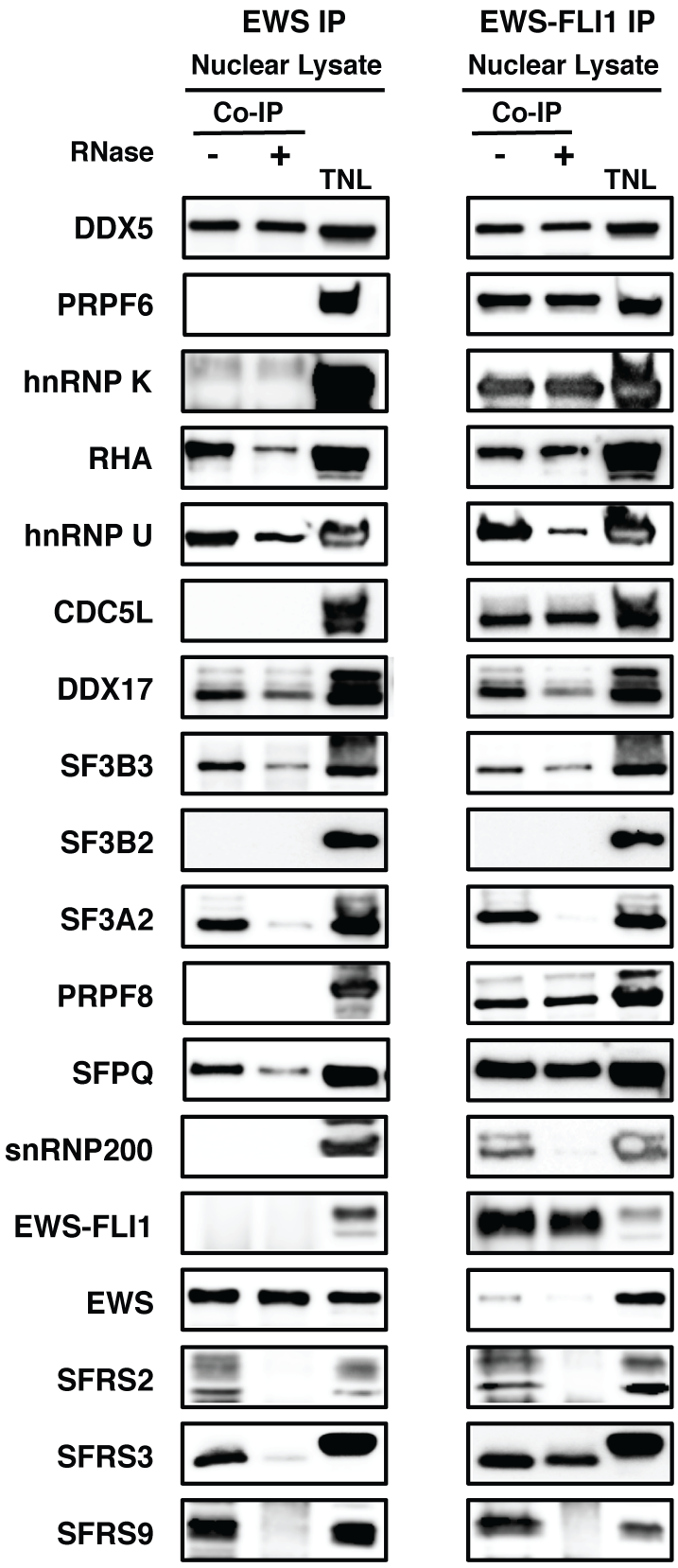

Fig. S2B. Experimental Validation of RNA Dependent or Independent EWS-FLI1 Associated Spliceosomal Complex Proteins by Co-IP. Antibodies used for the co-IP are indicated on the top and antibodies used for the western blots are indicated on the left. Samples were treated with or without RNase, washed and bound proteins were eluted and analyzed by 10% SDS-PAGE. Corresponding antibody pull downs showing the presence of proteins as a part of the complex without RNase treatment (lane 1), with RNase treatment (lane 2) and 10% of total nuclear lysate (TNL) was used as input (lane 3).

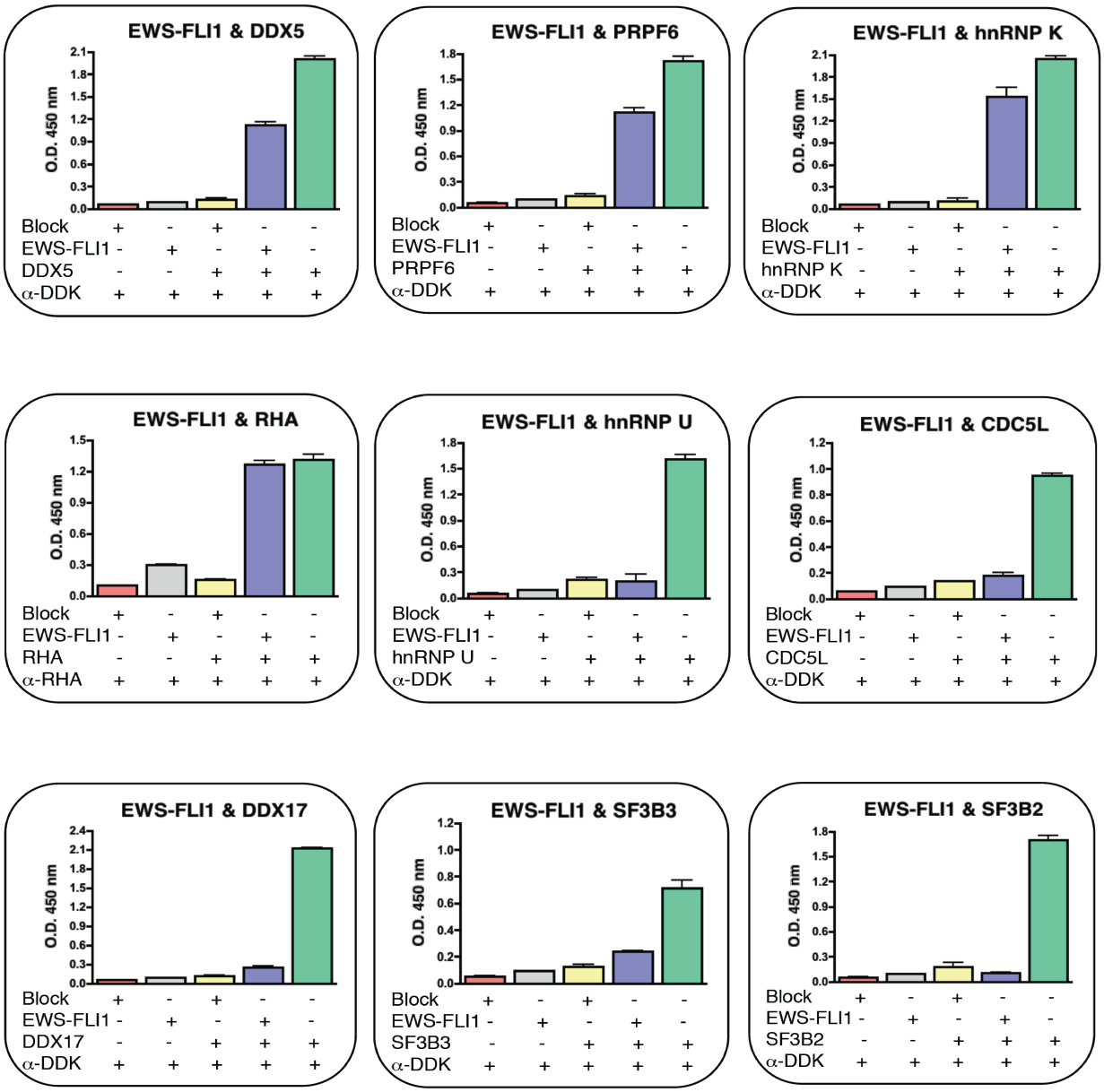

Fig. S3. EWS-FLI1 Direct Binding Partners of Spliceosome Proteins by ELISA. EWS-FLI1 protein was coated on the surface of the ELISA plate and specific protein interaction using anti-DDK monoclonal antibody with HRP. EWS-FLI1 protein alone followed by secondary antibody (grey bar), and blocking agent with their corresponding ligands followed by secondary antibody (yellow bar). For the positive control, ELISA plate wells were coated with their corresponding spliceosomal proteins and their secondary antibody (green bar). Specific protein-protein interactions are shown in blue bar. Error bars show mean ± SD from three individual experiments.

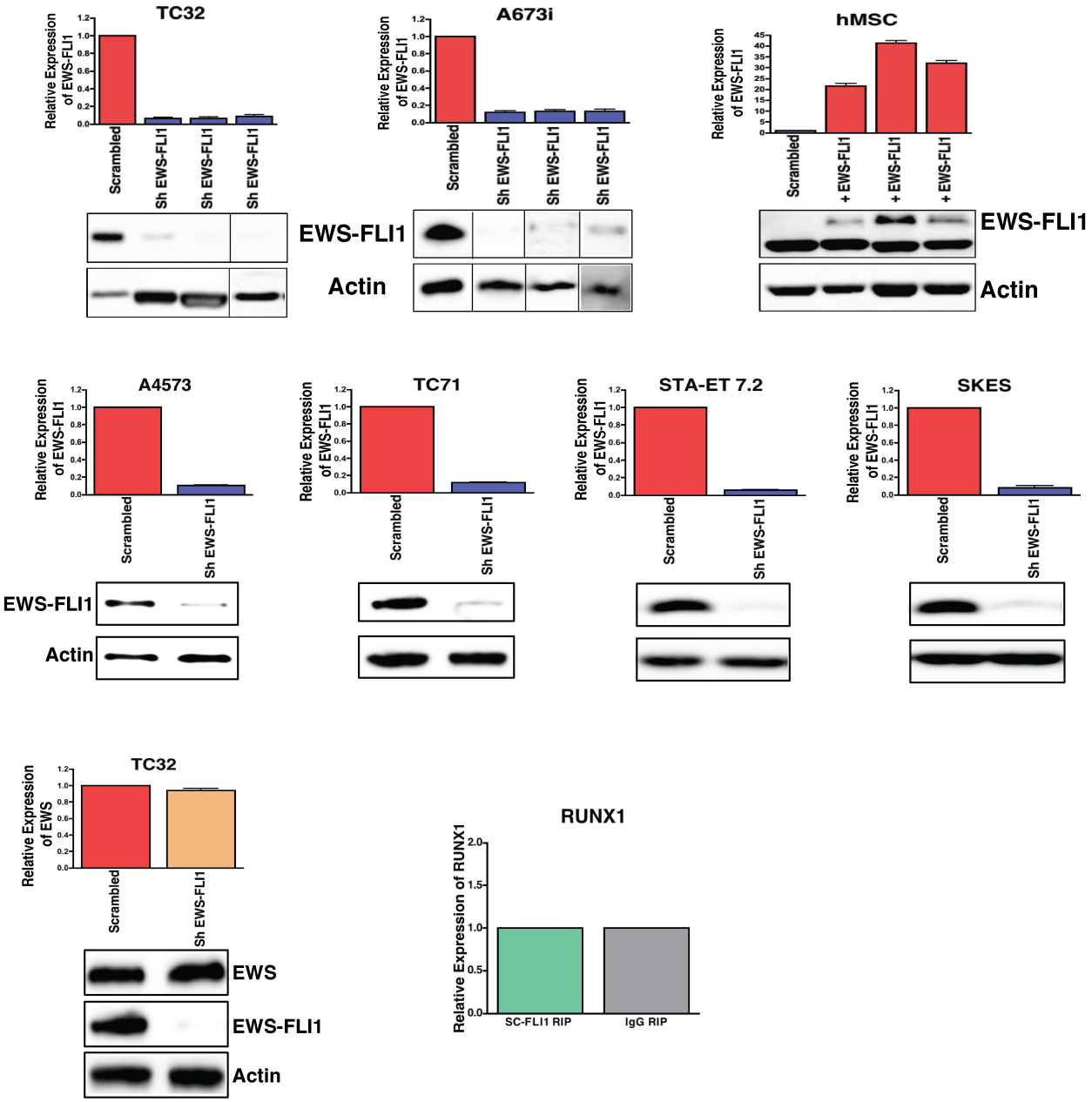

Fig. S4A. EWS-FLI1 shRNA Reduction or Overexpression Models Used for Exon Array Experiments and Validations. Reduction of EWS-FLI1 using shRNA in ES cell lines TC32, A673i, A4573, TC71, STA-ET 7.2 and SKES and exogenous expression of EWS-FLI1 in hMSC models used for exon array experiments and validations are shown. Each of these models was created in triplicate with qRT-PCR confirming the reduction (blue) or expression, scrambled shRNA transfected (red) of EWS-FLI1 mRNA shown on the top. Bottom panels showing the immunoblots confirming the reduction or expression of EWS-FLI1 protein. Actin was used as a loading control. Wild-type EWS expression in TC32 scrambled and shRNA reduced EWS-FLI1 by qRT-PCR and immunoblots are shown. The right lower panel shows the relative presence RUNX1 as a negative control for the RIP.

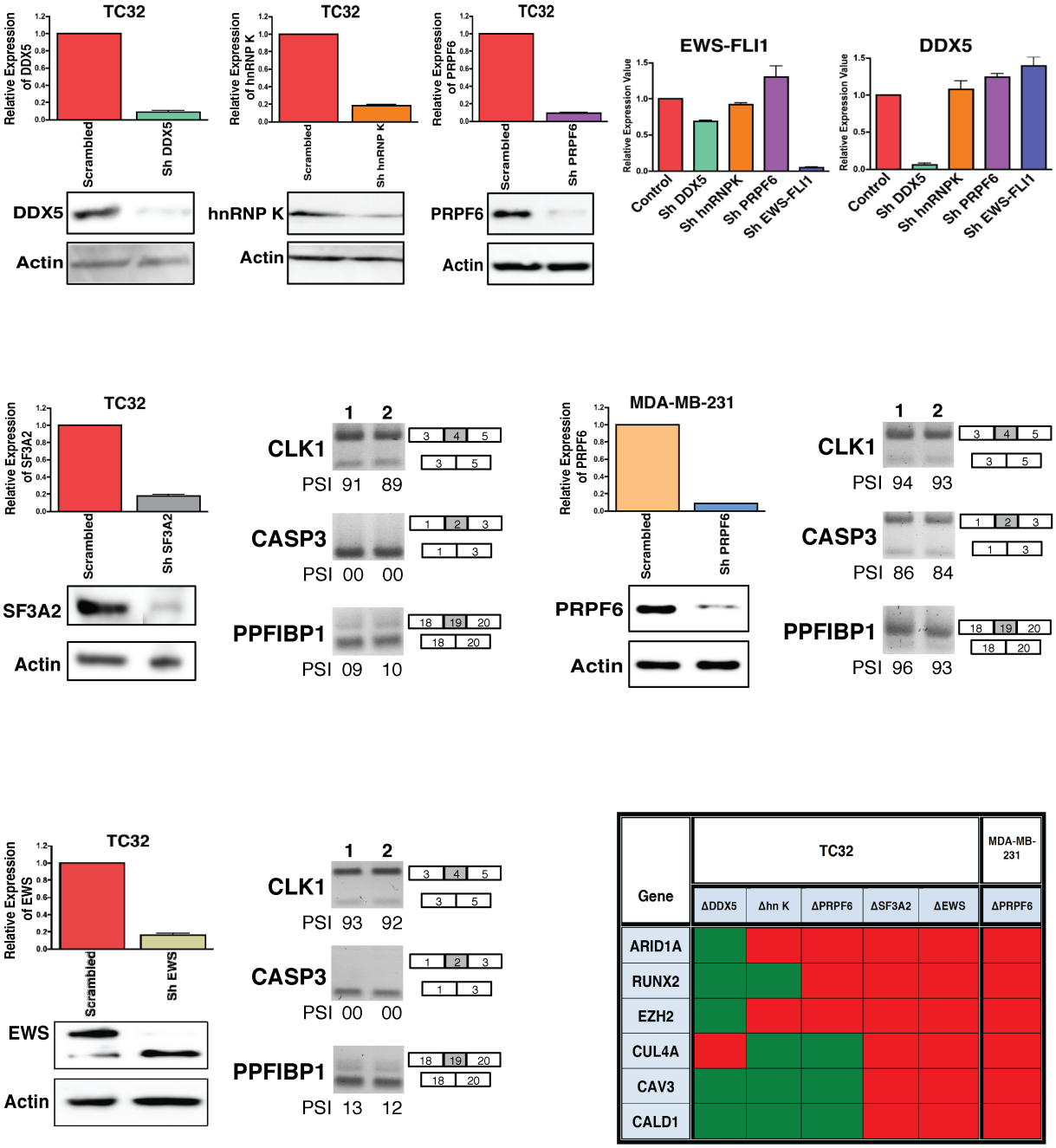

Fig. S4B. shRNA Reduction of Various Spliceosomal Protein Models and their isoform specific Expressions. shRNA reduction of EWS-FLI1 direct binding partners of spliceosomal proteins, DDX5, hnRNP K and PRPF6 in TC32 cells were shown. qRT-PCR and immunoblots confirming the reduction of DDX5, hnRNP K and PRPF6 are shown and actin was used as a loading control. The expression profiles of EWS-FLI1 and DDX5 in various protein shRNA reduction cells in TC32 are shown. As control for specificity, SF3A2 and EWS was reduced in TC32 and PRPF6 was reduced in MDA-MB-231 breast cancer cells. qRT-PCR and immunoblot confirming the reduction of genes was shown. On the right, PCR products associated with each splicing events are included. PSI of exon inclusion are shown below each lane. An overall summary table of specific isoform switches based upon various spliceosomal knockdowns are shown. Genes with EWS-FLI1 exon-specific isoform switch, similar to EWS-FLI1-green, no isoform switch-red.

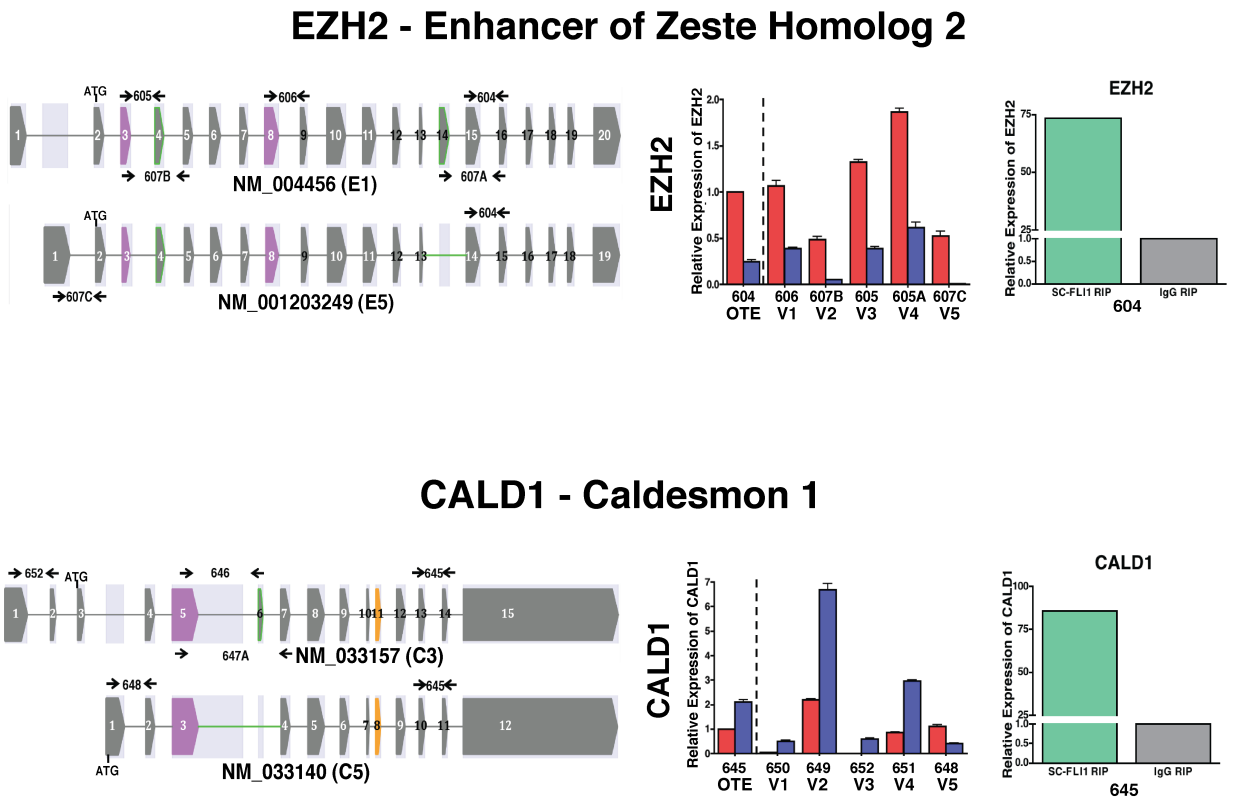

Fig. S4C. Alternatively Spliced Genes by EWS-FLI1 Impact Diverse Cellular Processes. Isoform specific *EZH2* and *CALD1,* qRT-PCR primer locations are indicated by forward and reverse arrow with specific primer number. Exons are indicated by grey or purple boxes, exon specific splice changes are coded as follows: alternative 5' splice site selection (purple), alternative 3' splice site (orange) or skipped exon (green line). Light blue boxes show the locations of exons present in other isoforms. qRT-PCR relative exon-specific expression of *EZH2* and *CALD1* by showing the fold expressions of qRT-PCR products based upon overall transcript expression (OTE) and exon specific transcript expression. RNA Immunoprecipitation (RIP) showing the relative presence of *EZH2* and *CALD1* message in FLI1 antibody IP compared to total 18S vs. IgG control IP.

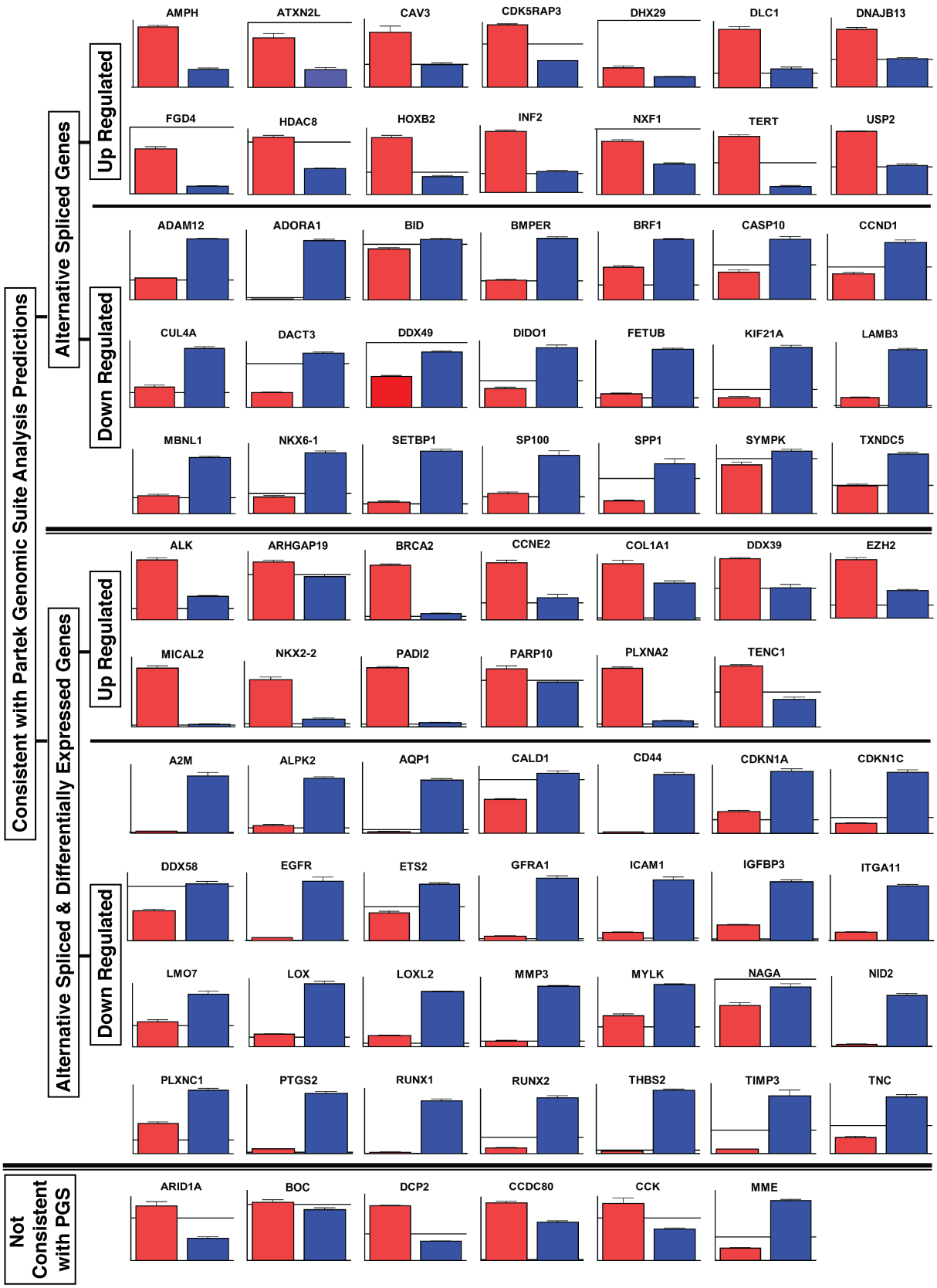

Fig. S5. Validations of AS Exon Behavior for 82 genes by qRT-PCR. Genes are listed along with relative expression levels by qRT-PCR for the selected exons from TC32 control (red) and

EWS-FLI1 reduced cells (blue). Based upon Affymetrix annotation of the exon array probeset loci, primers were designed to validate the AS exon behavior. Common primer sets were designed from unaltered regions of each genes were used for normalization and indicated as solid horizontal black line (set at y = 1). The scale on each graph is different based upon overall relative expression of the amplified transcript sections. Among 82 genes, 35 genes show only AS genes, top half, and 41 genes are both AS and differentially expressed, bottom half. Six genes on the bottom did not corroborate by qRT-PCR. The top and bottom sections are subdivided into up or down regulated transcripts which are consistent with PGS predicted exon behaviors.

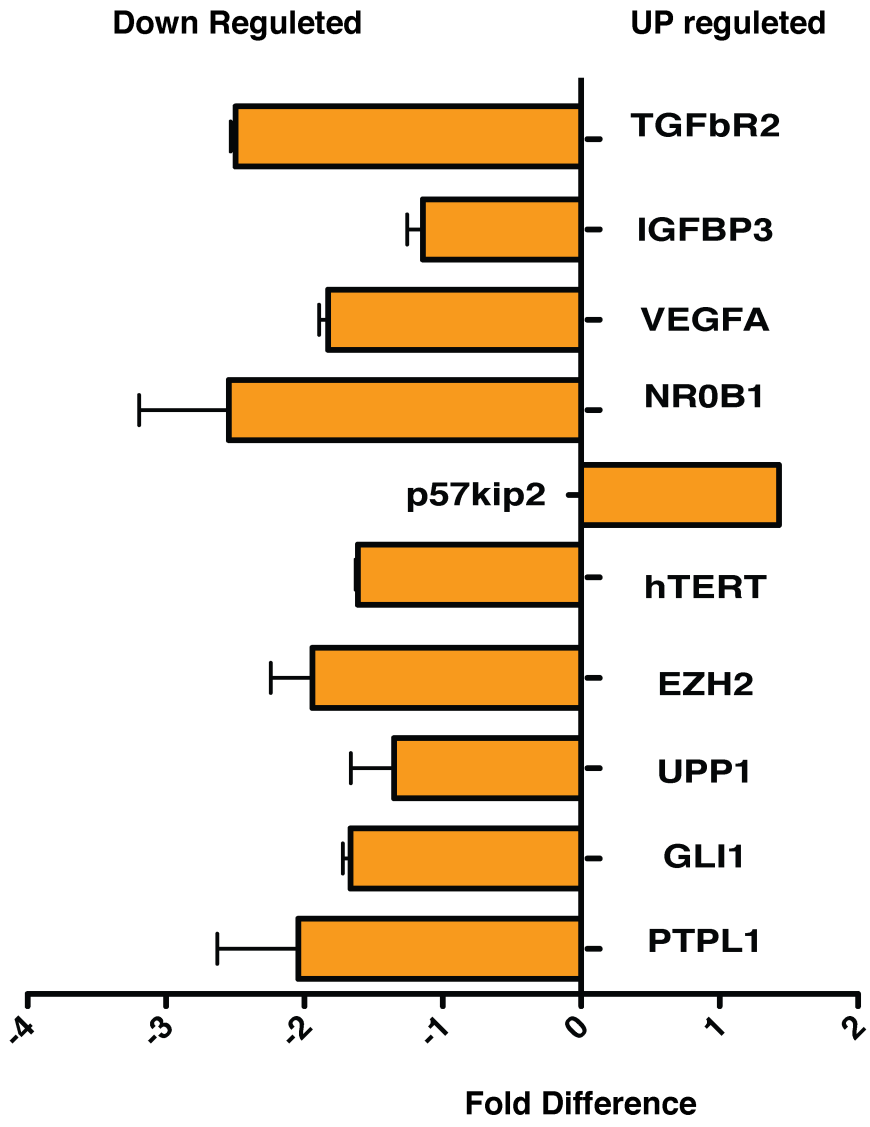

Fig. S6. YK-4-279 Treatment Effect on EWS-FLI1 Target Genes in TC71 Cells. qRT-PCR showing the relative expression of EWS-FLI1 target genes in YK-4-279 treated TC71 cells.

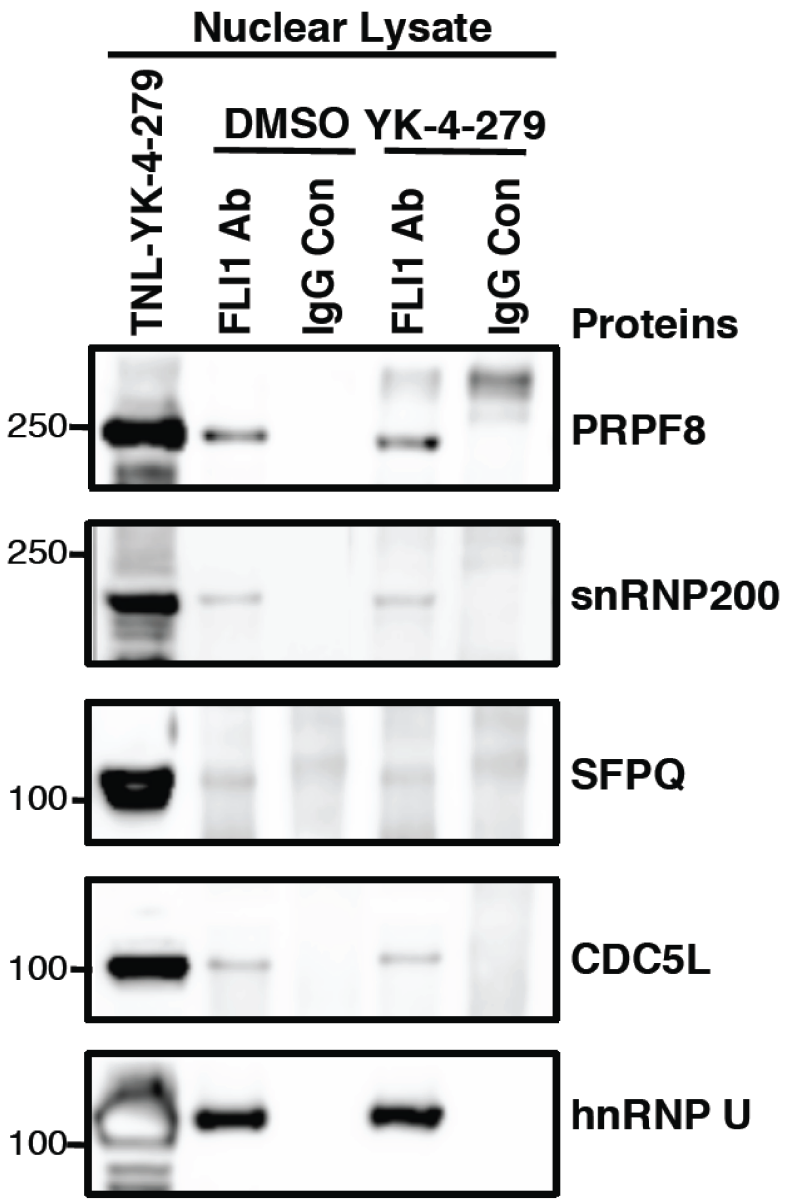

Fig. S7. YK-4-279 Treatment Effect on EWS-FLI1 Spliceosomal Complex Proteins. TC32 cells were treated with DMSO or YK-4-279 for 15hrs followed by isolation of total nuclear lysate (TNL) and subsequently co-IP experiments. YK-4-279 treated TNL (10%) was used as input (lane 1), FLI1 antibody precipitated proteins are shown for both DMSO (lane 2) and YK-4-279 (lane 4) treated cells. For the negative control, rabbit polyclonal IgG antibody (Ab) was used to confirm specificity (lanes 3 and 5). Antibodies for protein detection are to the right of the panels.

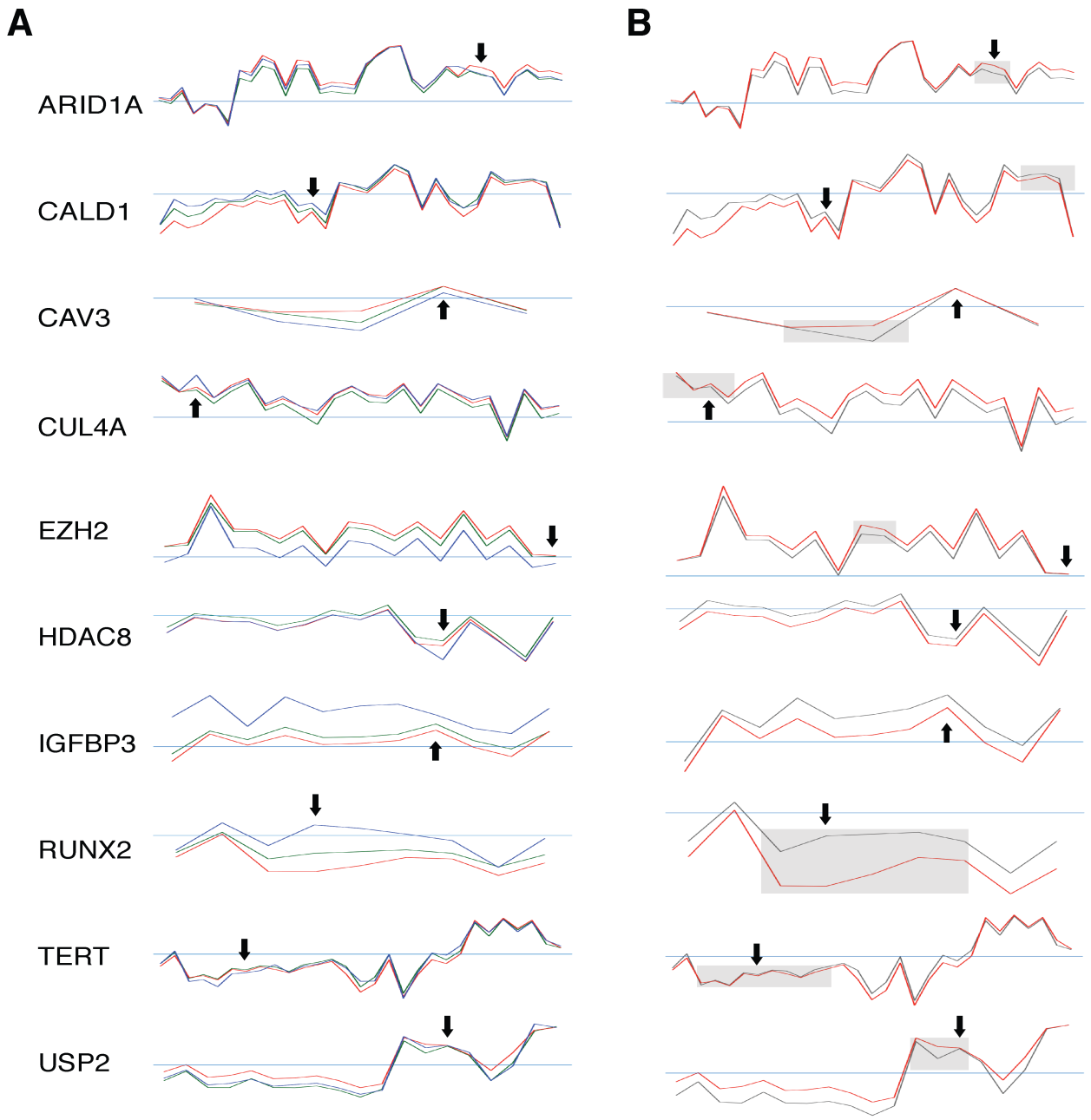

Fig. S8. Analysis of Specific Exon Expression Levels Based upon Probe-sets Spaced Along the Length of the Gene. (A) Gene-normalized exon expressions plotted for TC32 control (red), TC32 with reduced EWS-FLI1 (blue), and ESTS (green). Arrows indicate the loci that show alternative splicing. (B) Plots comparing gene-normalized exon expression in TC32 (red) and MDA-MB-231 (grey) showing important differences at specific regions (grey boxes) demonstrating the isoform-specific differences between ES and breast cancer. See Fig. 2 legend for additional detail.

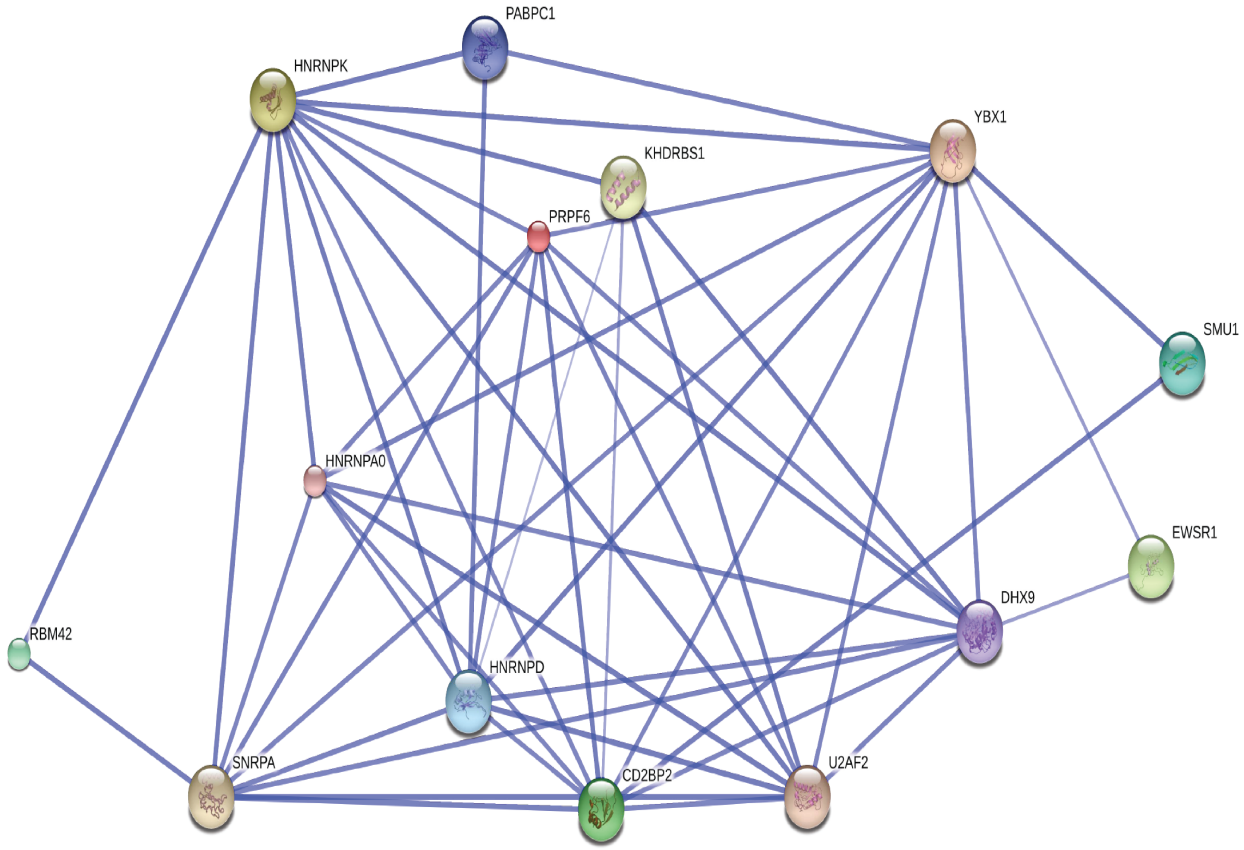

Fig. S9. STRING Analysis of EWS / YB1. STRING 9.1 analysis showing the EWS network interactions between various splicing protein partners and YB-1.

Table S1. LC-MS/MS identified potential protein participants in EWS-FLI1 complexes.

Proteins	Accession Number	Protein Description
1433F	Q04917	14-3-3 protein eta
1433G	P61981	14-3-3 protein gamma
2AAA	P30153	Serine/threonine-protein phosphatase 2A 65 kDa regulatory subunit A alpha isoform
ABCE1	P61221	ATP-binding cassette sub-family E member 1
ABCF1	Q8NE71	ATP-binding cassette sub-family F member 1
ACINU	Q9UKV3	Apoptotic chromatin condensation inducer in the nucleus
ACL6A	O96019	Actin-like protein 6A
ACLY	P53396	ATP-citrate synthase
ACTG	P63261	Actin, cytoplasmic 2
ACTN4	O43707	Alpha-actinin-4
ADDA	P35611	Alpha-adducin
ADPPT	Q9NRN7	L-aminoadipate-semialdehyde dehydrogenase-phosphopantetheinyl transferase
ALDOA	P04075	Fructose-bisphosphate aldolase A
ANM1	Q99873	Protein arginine N-methyltransferase 1
ANX11	P50995	Annexin A11
ANXA1	P04083	Annexin A1
ANXA2	P07355	Annexin A2
ANXA6	P08133	Annexin A6
APC4	Q9UJX5	Anaphase-promoting complex subunit 4
APC7	Q9UJX3	Anaphase-promoting complex subunit 7
APEX1	P27695	DNA-(apurinic or apyrimidinic site) lyase
API5	Q9BZZ5	Apoptosis inhibitor 5
ARHG1	Q92888	Rho guanine nucleotide exchange factor 1
ARHG2	Q92974	Rho guanine nucleotide exchange factor 2
ARI1B	Q8NFD5	AT-rich interactive domain-containing protein 1B
ARID1A	O14497	AT-rich interactive domain-containing protein 1A
ARID2	Q68CP9	AT-rich interactive domain-containing protein 2
ARK72	O43488	Aflatoxin B1 aldehyde reductase member 2
ARPC3	O15145	Actin-related protein 2/3 complex subunit 3
ASNS	P08243	Asparagine synthetase [glutamine-hydrolyzing]
AT2A2	P16615	Sarcoplasmic/endoplasmic reticulum calcium ATPase 2
ATX1	P54253	Ataxin-1
ATX2L	Q8WWM7	Ataxin-2-like protein
BAT3	P46379	Large proline-rich protein BAT3
BAZ1B	Q9UIG0	Tyrosine-protein kinase BAZ1B
BOLA2	Q9H3K6	BolA-like protein 2
BRK1	Q8WUW1	Probable protein BRICK1
C1TC	P11586	C-1-tetrahydrofolate synthase, cytoplasmic
CALX	P27824	Calnexin
CAND1	Q86VP6	Cullin-associated NEDD8-dissociated protein 1
CAP1	Q01518	Adenylyl cyclase-associated protein 1
CAPR1	Q14444	Caprin-1
CAPZB	P47756	F-actin-capping protein subunit beta
CAR11	Q9BXL7	Caspase recruitment domain-containing protein 11
CCAR1	Q8IX12	Cell division cycle and apoptosis regulator protein 1
CCNB1	P14635	G2/mitotic-specific cyclin-B1

CDC23	Q9UJX2	Cell division cycle protein 23 homolog
CDC5L	Q99459	Cell division cycle 5-like protein
CDC73	Q6P1J9	Parafibromin
CDK1	P06493	Cell division protein kinase 1
CG026	Q96N11	Uncharacterized protein C7orf26
CH60	P10809	60 kDa heat shock protein, mitochondrial
CHD1L	Q86WJ1	Chromodomain-helicase-DNA-binding protein 1-like
CHD4	Q14839	Chromodomain-helicase-DNA-binding protein 4
CHD8	Q9HCK8	Chromodomain-helicase-DNA-binding protein 8
CHERP	Q8IWX8	Calcium homeostasis endoplasmic reticulum protein
CKAP5	Q14008	Cytoskeleton-associated protein 5
CKS1	P61024	Cyclin-dependent kinases regulatory subunit 1
CLCA	P09496	Clathrin light chain A
CLH1	Q00610	Clathrin heavy chain 1
CNBP	P62633	Cellular nucleic acid-binding protein
CND3	Q9BPX3	Condensin complex subunit 3
CNDP2	Q96KP4	Cytosolic non-specific dipeptidase
CNOT1	A5YKK6	CCR4-NOT transcription complex subunit 1
COASY	Q13057	Bifunctional coenzyme A synthase
COPA	P53621	Coatomer subunit alpha
COPD	P48444	Coatomer subunit delta
COPG	Q9Y678	Coatomer subunit gamma
COR1B	Q9BR76	Coronin-1B
COR1C	Q9ULV4	Coronin-1C
CPNE1	Q99829	Copine-1
CPSF1	Q10570	Cleavage and polyadenylation specificity factor subunit 1
CPSF6	Q16630	Cleavage and polyadenylation specificity factor subunit 6
CRIP2	P52943	Cysteine-rich protein 2
CS010	Q969H8	UPF0556 protein C19orf10
CSDE1	O75534	Cold shock domain-containing protein E1
CSK21	P68400	Casein kinase II subunit alpha
CSN1	Q13098	COP9 signalosome complex subunit 1
CSN8	Q99627	COP9 signalosome complex subunit 8
CSRP1	P21291	Cysteine and glycine-rich protein 1
CSTF2	P33240	Cleavage stimulation factor subunit 2
CTBP1	Q13363	C-terminal-binding protein 1
CUL1	Q13616	Cullin-1
CUL3	Q13618	Cullin-3
CUL5	Q93034	Cullin-5
CV028	Q9Y3I0	UPF0027 protein C22orf28
DCTP1	Q9H773	dCTP pyrophosphatase 1
DD19A	Q9NUU7	ATP-dependent RNA helicase DDX19A
DDB1	Q16531	DNA damage-binding protein 1
DDX1	Q92499	ATP-dependent RNA helicase DDX1
DDX17	Q92841	Probable ATP-dependent RNA helicase DDX17
DDX18	Q9NVP1	ATP-dependent RNA helicase DDX18
DDX21	Q9NR30	Nucleolar RNA helicase 2
DDX23	Q9BUQ8	Probable ATP-dependent RNA helicase DDX23
DDX24	Q9GZR7	ATP-dependent RNA helicase DDX24
DDX39	O00148	ATP-dependent RNA helicase DDX39
DDX3X	O00571	ATP-dependent RNA helicase DDX3X
DDX42	Q86XP3	ATP-dependent RNA helicase DDX42

DDX46	Q7L014	Probable ATP-dependent RNA helicase DDX46
DDX5	P17844	Probable ATP-dependent RNA helicase DDX5
DDX50	Q9BQ39	ATP-dependent RNA helicase DDX50
DDX52	Q9Y2R4	Probable ATP-dependent RNA helicase DDX52
DHX15	O43143	Putative pre-mRNA-splicing factor ATP-dependent RNA helicase DHX15
DHX9	Q08211	ATP-dependent RNA helicase A
DKC1	O60832	H/ACA ribonucleoprotein complex subunit 4
DLRB1	Q9NP97	Dynein light chain roadblock-type 1
DNMT1	P26358	DNA (cytosine-5)-methyltransferase 1
DOCK7	Q96N67	Dedicator of cytokinesis protein 7
DPYL2	Q16555	Dihydropyrimidinase-related protein 2
DRG1	Q9Y295	Developmentally-regulated GTP-binding protein 1
DSRAD	P55265	Double-stranded RNA-specific adenosine deaminase
DYHC1	Q14204	Cytoplasmic dynein 1 heavy chain 1
EDF1	O60869	Endothelial differentiation-related factor 1
EF1A1	P68104	Elongation factor 1-alpha 1
EF1A3	Q5VTE0	Putative elongation factor 1-alpha-like 3
EF1B	P24534	Elongation factor 1-beta
EF1D	P29692	Elongation factor 1-delta
EF1G	P26641	Elongation factor 1-gamma
EF2	P13639	Elongation factor 2
EHD1	Q9H4M9	EH domain-containing protein 1
EI2BD	Q9UI10	Translation initiation factor eIF-2B subunit delta
EI2BE	Q13144	Translation initiation factor eIF-2B subunit epsilon
EIF3A	Q14152	Eukaryotic translation initiation factor 3 subunit A
EIF3B	P55884	Eukaryotic translation initiation factor 3 subunit B
EIF3C	Q99613	Eukaryotic translation initiation factor 3 subunit C
EIF3D	O15371	Eukaryotic translation initiation factor 3 subunit D
EIF3L	Q9Y262	Eukaryotic translation initiation factor 3 subunit L
EIF3M	Q7L2H7	Eukaryotic translation initiation factor 3 subunit M
ELAV1	Q15717	ELAV-like protein 1
ENPL	P14625	Endoplasmin
ERF1	P62495	Eukaryotic peptide chain release factor subunit 1
ERF3A	P15170	Eukaryotic peptide chain release factor GTP-binding subunit ERF3A
ERF3B	Q8IYD1	Eukaryotic peptide chain release factor GTP-binding subunit ERF3B
EST1	P23141	Liver carboxylesterase 1
ESYT1	Q9BSJ8	Extended synaptotagmin-1
EWS	Q01844	RNA-binding protein EWS
EXOS4	Q9NPD3	Exosome complex exonuclease RRP41
EXOS5	Q9NQT4	Exosome complex exonuclease RRP46
EXOSX	Q01780	Exosome component 10
EZRI	P15311	Ezrin
FAS	P49327	Fatty acid synthase
FBRL	P22087	rRNA 2'-O-methyltransferase fibrillarin
FFR	Q9UID3	Protein fat-free homolog
FLI1	Q01543	Friend leukemia integration 1 transcription factor
FLIP1	Q7Z7B0	Filamin-A-interacting protein 1
FLNA	P21333	Filamin-A
FLNB	O75369	Filamin-B
FSCN1	Q16658	Fascin
FUBP1	Q96AE4	Far upstream element-binding protein 1

FUBP2	Q92945	Far upstream element-binding protein 2
FUS	P35637	RNA-binding protein FUS
G3BP1	Q13283	Ras GTPase-activating protein-binding protein 1
G3BP2	Q9UN86	Ras GTPase-activating protein-binding protein 2
G3P	P04406	Glyceraldehyde-3-phosphate dehydrogenase
G6PD	P11413	Glucose-6-phosphate 1-dehydrogenase
G6PI	P06744	Glucose-6-phosphate isomerase
GABPA	Q06546	GA-binding protein alpha chain
GANAB	Q14697	Neutral alpha-glucosidase AB
GBRL2	P60520	Gamma-aminobutyric acid receptor-associated protein-like 2
GCN1L	Q92616	Translational activator GCN1
GLU2B	P14314	Glucosidase 2 subunit beta
GNL3	Q9BVP2	Guanine nucleotide-binding protein-like 3
GRIN1	Q7Z2K8	G protein-regulated inducer of neurite outgrowth 1
GSLG1	Q92896	Golgi apparatus protein 1
GTF2I	P78347	General transcription factor II-I
GUAA	P49915	GMP synthase [glutamine-hydrolyzing]
H12	P16403	Histone H1.2
H1X	Q92522	Histone H1x
H2A1C	Q93077	Histone H2A type 1-C
H2A2A	Q6FI13	Histone H2A type 2-A
H2B1L	Q99880	Histone H2B type 1-L
H4	P62805	Histone H4
HAP28	Q13442	28 kDa heat- and acid-stable phosphoprotein
HCFC1	P51610	Host cell factor 1
HDAC2	Q92769	Histone deacetylase 2
HINT1	P49773	Histidine triad nucleotide-binding protein 1
HMGB1	P09429	High mobility group protein B1
HMGB2	P26583	High mobility group protein B2
HN1L	Q9H910	Hematological and neurological expressed 1-like protein
HNRH1	P31943	Heterogeneous nuclear ribonucleoprotein H
HNRH3	P31942	Heterogeneous nuclear ribonucleoprotein H3
HNRL1	Q9BUJ2	Heterogeneous nuclear ribonucleoprotein U-like protein 1
HNRL2	Q1KMD3	Heterogeneous nuclear ribonucleoprotein U-like protein 2
HNRPC	P07910	Heterogeneous nuclear ribonucleoproteins C1/C2
HNRPD	Q14103	Heterogeneous nuclear ribonucleoprotein D0
HNRPG	P38159	Heterogeneous nuclear ribonucleoprotein G
HNRPK	P61978	Heterogeneous nuclear ribonucleoprotein K
HNRPL	P14866	Heterogeneous nuclear ribonucleoprotein L
HNRPQ	O60506	Heterogeneous nuclear ribonucleoprotein Q
HNRPR	O43390	Heterogeneous nuclear ribonucleoprotein R
HNRPU	Q00839	Heterogeneous nuclear ribonucleoprotein U
HS105	Q92598	Heat shock protein 105 kDa
HS90A	P07900	Heat shock protein HSP 90-alpha
HS90B	P08238	Heat shock protein HSP 90-beta
HSP71	P08107	Heat shock 70 kDa protein 1A/1B
HSP7C	P11142	Heat shock cognate 71 kDa protein
HSP7E	Q0VDF9	Heat shock 70 kDa protein 14
HSPB1	P04792	Heat shock protein beta-1
HUWE1	Q7Z6Z7	E3 ubiquitin-protein ligase HUWE1
HXK1	P19367	Hexokinase-1
IF16	Q16666	Gamma-interferon-inducible protein 16

IF2A	P05198	Eukaryotic translation initiation factor 2 subunit 1
IF2B1	Q9NZI8	Insulin-like growth factor 2 mRNA-binding protein 1
IF2P	O60841	Eukaryotic translation initiation factor 5B
IF4A1	P60842	Eukaryotic initiation factor 4A-I
IF5	P55010	Eukaryotic translation initiation factor 5
IF5A1	P63241	Eukaryotic translation initiation factor 5A-1
ILF2	Q12905	Interleukin enhancer-binding factor 2
ILF3	Q12906	Interleukin enhancer-binding factor 3
IMA1	P52294	Importin subunit alpha-1
IMA2	P52292	Importin subunit alpha-2
IMA3	O00505	Importin subunit alpha-3
IMA4	O00629	Importin subunit alpha-4
IMB1	Q14974	Importin subunit beta-1
IMDH2	P12268	Inosine-5'-monophosphate dehydrogenase 2
INO80	Q9ULG1	Putative DNA helicase INO80 complex homolog 1
INT2	Q9H0H0	Integrator complex subunit 2
INT3	Q68E01	Integrator complex subunit 3
INT4	Q96HW7	Integrator complex subunit 4
INT5	Q6P9B9	Integrator complex subunit 5
INT6	Q9UL03	Integrator complex subunit 6
IPO5	O00410	Importin-5
IPO7	O95373	Importin-7
IPYR	Q15181	Inorganic pyrophosphatase
JKIP3	Q5VZ66	Janus kinase and microtubule-interacting protein 3
K0895	Q8NCT3	Uncharacterized protein KIAA0895
K1967	Q8N163	Protein KIAA1967
K6PP	Q01813	6-phosphofructokinase type C
KDM1A	O60341	Lysine-specific histone demethylase 1A
KHDR1	Q07666	KH domain-containing, RNA-binding, signal transduction-associated protein 1
KI67	P46013	Antigen KI-67
KIF2A	O00139	Kinesin-like protein KIF2A
KINH	P33176	Kinesin-1 heavy chain
KLF16	Q9BXK1	Krueppel-like factor 16
KPYM	P14618	Pyruvate kinase isozymes M1/M2
LA	P05455	Lupus La protein
LAP2A	P42166	Lamina-associated polypeptide 2, isoform alpha
LRC47	Q8N1G4	Leucine-rich repeat-containing protein 47
MAP4	P27816	Microtubule-associated protein 4
MAT2B	Q9NZL9	Methionine adenosyltransferase 2 subunit beta
MATR3	P43243	Matrin-3
MBB1A	Q9BQG0	Myb-binding protein 1A
MCM2	P49736	DNA replication licensing factor MCM2
MCM4	P33991	DNA replication licensing factor MCM4
MCM5	P33992	DNA replication licensing factor MCM5
MCM7	P33993	DNA replication licensing factor MCM7
MDC1	Q14676	Mediator of DNA damage checkpoint protein 1
ML12A	P19105	Myosin regulatory light chain 12A
MPP2	Q14168	MAGUK p55 subfamily member 2
MRE11	P49959	Double-strand break repair protein MRE11A
MRT4	Q9UKD2	mRNA turnover protein 4 homolog
MTL13	Q8N6R0	Methyltransferase-like protein 13

MYH10	P35580	Myosin-10
MYH9	P35579	Myosin-9
MYL6	P60660	Myosin light polypeptide 6
NACA	Q13765	Nascent polypeptide-associated complex subunit alpha
NADAP	Q9BWU0	Kanadaptin
NAT10	Q9H0A0	N-acetyltransferase 10
NBN	O60934	Nibrin
NCBP1	Q09161	Nuclear cap-binding protein subunit 1
NDKA	P15531	Nucleoside diphosphate kinase A
NELFB	Q8WX92	Negative elongation factor B
NFRKB	Q6P4R8	Nuclear factor related to kappa-B-binding protein
NIBL1	Q96TA1	Niban-like protein 1
NOC2L	Q9Y3T9	Nucleolar complex protein 2 homolog
NOL6	Q9H6R4	Nucleolar protein 6
NONO	Q15233	Non-POU domain-containing octamer-binding protein
NOP2	P46087	Putative ribosomal RNA methyltransferase NOP2
NOP56	O00567	Nucleolar protein 56
NOP58	Q9Y2X3	Nucleolar protein 58
NPL4	Q8TAT6	Nuclear protein localization protein 4 homolog
NPM	P06748	Nucleophosmin
NPM3	O75607	Nucleoplasmin-3
NUCL	P19338	Nucleolin
NUMA1	Q14980	Nuclear mitotic apparatus protein 1
OGT1	O15294	UDP-N-acetylglucosamine--peptide N-acetylglucosaminyltransferase
ORC5	O43913	Origin recognition complex subunit 5
OSBL8	Q9BZF1	Oxysterol-binding protein-related protein 8
PA1B2	P68402	Platelet-activating factor acetylhydrolase IB subunit beta
PA1B3	Q15102	Platelet-activating factor acetylhydrolase IB subunit gamma
PA2G4	Q9UQ80	Proliferation-associated protein 2G4
PABP1	P11940	Polyadenylate-binding protein 1
PABP2	Q86U42	Polyadenylate-binding protein 2
PAPS1	O43252	Bifunctional 3'-phosphoadenosine 5'-phosphosulfate synthase 1
PAR14	Q460N5	Poly [ADP-ribose] polymerase 14
PARP1	P09874	Poly [ADP-ribose] polymerase 1
PB1	Q86U86	Protein polybromo-1
PCBP1	Q15365	Poly(rC)-binding protein 1
PCBP2	Q15366	Poly(rC)-binding protein 2
PDC6I	Q8WUM4	Programmed cell death 6-interacting protein
PDCD4	Q53EL6	Programmed cell death protein 4
PDIA1	P07237	Protein disulfide-isomerase
PDIA3	P30101	Protein disulfide-isomerase A3
PDLI5	Q96HC4	PDZ and LIM domain protein 5
PDS5B	Q9NTI5	Sister chromatid cohesion protein PDS5 homolog B
PGM1	P36871	Phosphoglucomutase-1
PNKP	Q96T60	Bifunctional polynucleotide phosphatase/kinase
POP1	Q99575	Ribonucleases P/MRP protein subunit POP1
PP1G	P36873	Serine/threonine-protein phosphatase PP1-gamma catalytic subunit
PP1RA	Q96QC0	Serine/threonine-protein phosphatase 1 regulatory subunit 10
PP2AA	P67775	Serine/threonine-protein phosphatase 2A catalytic subunit alpha iso
PPIB	P23284	Peptidyl-prolyl cis-trans isomerase B
PPIH	O43447	Peptidyl-prolyl cis-trans isomerase H
PPIL1	Q9Y3C6	Peptidyl-prolyl cis-trans isomerase-like 1

PR40A	O75400	Pre-mRNA-processing factor 40 homolog A
PRDX1	Q06830	Peroxiredoxin-1
PRDX2	P32119	Peroxiredoxin-2
PRKDC	P78527	DNA-dependent protein kinase catalytic subunit
PRP6	O94906	Pre-mRNA-processing factor 6
PRP8	Q6P2Q9	Pre-mRNA-processing-splicing factor 8
PRPF3	O43395	U4/U6 small nuclear ribonucleoprotein Prp3
PRPS1	P60891	Ribose-phosphate pyrophosphokinase 1
PRS4	P62191	26S protease regulatory subunit 4
PSA7	O14818	Proteasome subunit alpha type-7
PSIP1	O75475	PC4 and SFRS1-interacting protein
PSMD1	Q99460	26S proteasome non-ATPase regulatory subunit 1
PSMD3	O43242	26S proteasome non-ATPase regulatory subunit 3
PSME3	P61289	Proteasome activator complex subunit 3
PSPC1	Q8WXF1	Paraspeckle component 1
PTBP1	P26599	Polypyrimidine tract-binding protein 1
PUF60	Q9UHX1	Poly(U)-binding-splicing factor PUF60
PUR2	P22102	Trifunctional purine biosynthetic protein adenosine-3
PYR1	P27708	CAD protein
PYR5	P11172	Uridine 5'-monophosphate synthase
QKI	Q96PU8	Protein quaking
RA1L3	P0C7M2	Putative heterogeneous nuclear ribonucleoprotein A1-like 3
RAB35	Q15286	Ras-related protein Rab-35
RADI	P35241	Radixin
RAGP1	P46060	Ran GTPase-activating protein 1
RANG	P43487	Ran-specific GTPase-activating protein
RBBP7	Q16576	Histone-binding protein RBBP7
RBM10	P98175	RNA-binding protein 10
RBM25	P49756	RNA-binding protein 25
RBM3	P98179	Putative RNA-binding protein 3
RBM39	Q14498	RNA-binding protein 39
RCC2	Q9P258	Protein RCC2
RCOR1	Q9UKL0	REST corepressor 1
RECQ1	P46063	ATP-dependent DNA helicase Q1
REQU	Q92785	Zinc finger protein ubi-d4
RIF1	Q5UIP0	Telomere-associated protein RIF1
RL12	P30050	60S ribosomal protein L12
RL13	P26373	60S ribosomal protein L13
RL17	P18621	60S ribosomal protein L17
RL18	Q07020	60S ribosomal protein L18
RL1D1	O76021	Ribosomal L1 domain-containing protein 1
RL22	P35268	60S ribosomal protein L22
RL23	P62829	60S ribosomal protein L23
RL23A	P62750	60S ribosomal protein L23a
RL27	P61353	60S ribosomal protein L27
RL27A	P46776	60S ribosomal protein L27a
RL29	P47914	60S ribosomal protein L29
RL30	P62888	60S ribosomal protein L30
RL31	P62899	60S ribosomal protein L31
RL36	Q9Y3U8	60S ribosomal protein L36
RL40	P62987	Ubiquitin-60S ribosomal protein L40
RL6	Q02878	60S ribosomal protein L6

RL7A	P62424	60S ribosomal protein L7a
RLA0	P05388	60S acidic ribosomal protein P0
RLA0L	Q8NHW5	60S acidic ribosomal protein P0-like
RLA1	P05386	60S acidic ribosomal protein P1
RLA2	P05387	60S acidic ribosomal protein P2
RO60	P10155	60 kDa SS-A/Ro ribonucleoprotein
ROA0	Q13151	Heterogeneous nuclear ribonucleoprotein A0
ROA1	P09651	Heterogeneous nuclear ribonucleoprotein A1
ROA2	P22626	Heterogeneous nuclear ribonucleoproteins A2/B1
ROA3	P51991	Heterogeneous nuclear ribonucleoprotein A3
ROCK2	O75116	Rho-associated protein kinase 2
RPA2	Q9H9Y6	DNA-directed RNA polymerase I subunit RPA2
RPAC1	O15160	DNA-directed RNA polymerases I and III subunit RPAC1
RPC3	Q9BUI4	DNA-directed RNA polymerase III subunit RPC3
RRP1B	Q14684	Ribosomal RNA processing protein 1 homolog B
RRP44	Q9Y2L1	Exosome complex exonuclease RRP44
RS10	P46783	40S ribosomal protein S10
RS12	P25398	40S ribosomal protein S12
RS14	P62263	40S ribosomal protein S14
RS16	P62249	40S ribosomal protein S16
RS18	P62269	40S ribosomal protein S18
RS19	P39019	40S ribosomal protein S19
RS2	P15880	40S ribosomal protein S2
RS20	P60866	40S ribosomal protein S20
RS23	P62266	40S ribosomal protein S23
RS24	P62847	40S ribosomal protein S24
RS25	P62851	40S ribosomal protein S25
RS26	P62854	40S ribosomal protein S26
RS27L	Q71UM5	40S ribosomal protein S27
RS28	P62857	40S ribosomal protein S28
RS3	P23396	40S ribosomal protein S3
RS30	P62861	40S ribosomal protein S30
RS3A	P61247	40S ribosomal protein S3a
RS5	P46782	40S ribosomal protein S5
RS6	P62753	40S ribosomal protein S6
RS8	P62241	40S ribosomal protein S8
RS9	P46781	40S ribosomal protein S9
RSMB	P14678	Small nuclear ribonucleoprotein-associated proteins B and B'
RSSA	P08865	40S ribosomal protein SA
RU17	P08621	U1 small nuclear ribonucleoprotein 70 kDa
RU2A	P09661	U2 small nuclear ribonucleoprotein A'
RUEL1	Q5VYJ4	Putative small nuclear ribonucleoprotein polypeptide E-like protein 1
RUVB1	Q9Y265	RuvB-like 1
RUVB2	Q9Y230	RuvB-like 2
RUXF	P62306	Small nuclear ribonucleoprotein F
RUXG	P62308	Small nuclear ribonucleoprotein G
SAFB1	Q15424	Scaffold attachment factor B1
SAHH	P23526	Adenosylhomocysteinase
SARNP	P82979	SAP domain-containing ribonucleoprotein
SC23A	Q15436	Protein transport protein Sec23A
SC24C	P53992	Protein transport protein Sec24C
SC31A	O94979	Protein transport protein Sec31A

SEC13	P55735	Protein SEC13 homolog
SEPT2	Q15019	Septin-2
SERPH	P50454	Serpin H1
SET	Q01105	Protein SET
SET1A	O15047	Histone-lysine N-methyltransferase SETD1A
SF01	Q15637	Splicing factor 1
SF3A1	Q15459	Splicing factor 3A subunit 1
SF3A2	Q15428	Splicing factor 3A subunit 1
SF3B1	O75533	Splicing factor 3B subunit 1
SF3B2	Q13435	Splicing factor 3B subunit 2
SF3B3	Q15393	Splicing factor 3B subunit 3
SF3B4	Q15427	Splicing factor 3B subunit 4
SFPQ	P23246	Splicing factor, proline- and glutamine-rich
SFR11	Q05519	Splicing factor, arginine/serine-rich 11
SFRS2	Q01130	Splicing factor, arginine/serine-rich 2
SFRS3	P84103	Splicing factor, arginine/serine-rich 3
SFRS9	Q13242	Splicing factor, arginine/serine-rich 9
SH3G1	Q99961	Endophilin-A2
SIN3A	Q96ST3	Paired amphipathic helix protein Sin3a
SK2L2	P42285	Superkiller viralicidic activity 2-like 2
SMAD4	Q13485	Mothers against decapentaplegic homolog 4
SMAP1	Q8IYB5	Stromal membrane-associated protein 1
SMC1A	Q14683	Structural maintenance of chromosomes protein 1A
SMC2	O95347	Structural maintenance of chromosomes protein 2
SMC4	Q9NTJ3	Structural maintenance of chromosomes protein 4
SMCA4	P51532	Transcription activator BRG1
SMCA5	O60264	SWI/SNF-related matrix-associated actin-dependent regulator of chromatin subfamily A member 5
SMD1	P62314	Small nuclear ribonucleoprotein Sm D1
SMD2	P62316	Small nuclear ribonucleoprotein Sm D2
SMD3	P62318	Small nuclear ribonucleoprotein Sm D3
SMRC1	Q92922	SWI/SNF complex subunit SMARCC1
SMRC2	Q8TAQ2	SWI/SNF complex subunit SMARCC2
SND1	Q7KZF4	Staphylococcal nuclease domain-containing protein 1
SNF5	Q12824	SWI/SNF-related matrix-associated actin-dependent regulator of chromatin subfamily B member 1
SNRPA	P09012	U1 small nuclear ribonucleoprotein A
SNUT1	O43290	U4/U6.U5 tri-snRNP-associated protein 1
SNUT2	Q53GS9	U4/U6.U5 tri-snRNP-associated protein 2
SNW1	Q13573	SNW domain-containing protein 1
SNX18	Q96RF0	Sorting nexin-18
SPF27	O75934	Pre-mRNA-splicing factor SPF27
SPS1	P49903	Selenide, water dikinase 1
SPS2	Q99611	Selenide, water dikinase 2
SPTA2	Q13813	Spectrin alpha chain, brain
SPTB2	Q01082	Spectrin beta chain, brain 1
SR140	O15042	U2-associated protein SR140
SRPK2	P78362	Serine/threonine-protein kinase SRPK2
SRRM2	Q9UQ35	Serine/arginine repetitive matrix protein 2
SRRT	Q9BXP5	Serrate RNA effector molecule homolog
SSRP1	Q08945	FACT complex subunit SSRP1
ST18	O60284	Suppression of tumorigenicity 18 protein

STAT1	P42224	Signal transducer and activator of transcription 1-alpha/beta
STIP1	P31948	Stress-induced-phosphoprotein 1
STK24	Q9Y6E0	Serine/threonine-protein kinase 24
STK35	Q8TDR2	Serine/threonine-protein kinase 35
STMN1	P16949	Stathmin
SUMO4	Q6EEV6	Small ubiquitin-related modifier 4
SYFB	Q9NSD9	Phenylalanyl-tRNA synthetase beta chain
SYIC	P41252	Isoleucyl-tRNA synthetase, cytoplasmic
SYNC	O43776	Asparaginyl-tRNA synthetase, cytoplasmic
SYQ	P47897	Glutaminyl-tRNA synthetase
SYSC	P49591	Seryl-tRNA synthetase, cytoplasmic
SYWC	P23381	Tryptophanyl-tRNA synthetase, cytoplasmic
SYYC	P54577	Tyrosyl-tRNA synthetase, cytoplasmic
T2FB	P13984	General transcription factor IIF subunit 2
TADBP	Q13148	TAR DNA-binding protein 43
TALDO	P37837	Transaldolase
TAU	P10636	Microtubule-associated protein tau
TBA1B	P68363	Tubulin alpha-1B chain
TBA1C	Q9BQE3	Tubulin alpha-1C chain
TBA3C	Q13748	Tubulin alpha-3C/D chain
TBA4A	P68366	Tubulin alpha-4A chain
TBB2C	P68371	Tubulin beta-2C chain
TBB3	Q13509	Tubulin beta-3 chain
TBB4	P04350	Tubulin beta-4 chain
TBB5	P07437	Tubulin beta chain
TBB6	Q9BUF5	Tubulin beta-6 chain
TBCD	Q9BTW9	Tubulin-specific chaperone D
TBL3	Q12788	Transducin beta-like protein 3
TCPA	P17987	T-complex protein 1 subunit alpha
TCPB	P78371	T-complex protein 1 subunit beta
TCPD	P50991	T-complex protein 1 subunit delta
TCPE	P48643	T-complex protein 1 subunit epsilon
TCPG	P49368	T-complex protein 1 subunit gamma
TCPH	Q99832	T-complex protein 1 subunit eta
TCPQ	P50990	T-complex protein 1 subunit theta
TCPZ	P40227	T-complex protein 1 subunit zeta
TCRG1	O14776	Transcription elongation regulator 1
TERA	P55072	Transitional endoplasmic reticulum ATPase
TF3C1	Q12789	General transcription factor 3C polypeptide 1
TF3C3	Q9Y5Q9	General transcription factor 3C polypeptide 3
TF3C4	Q9UKN8	General transcription factor 3C polypeptide 4
TF3C5	Q9Y5Q8	General transcription factor 3C polypeptide 5
TFG	Q92734	Protein TFG
TFR1	P02786	Transferrin receptor protein 1
THOC1	Q96FV9	THO complex subunit 1
THOC4	Q86V81	THO complex subunit 4
THOC5	Q13769	THO complex subunit 5 homolog
TIF1B	Q13263	Transcription intermediary factor 1-beta
TKT	P29401	Transketolase
TLN1	Q9Y490	Talin-1
TOE1	Q96GM8	Target of EGR1 protein 1
TOP1	P11387	DNA topoisomerase 1

TOP2B	Q02880	DNA topoisomerase 2-beta
TPM4	P67936	Tropomyosin alpha-4 chain
TPR	P12270	Nucleoprotein TPR
TRAP1	Q12931	Heat shock protein 75 kDa, mitochondrial
TRM1L	Q7Z2T5	TRM1-like protein
TRRAP	Q9Y4A5	Transformation/transcription domain-associated protein
TRY6	Q8NHM4	Putative trypsin-6
TSR1	Q2NL82	Pre-rRNA-processing protein TSR1 homolog
TTHY	P02766	Transthyretin
TWF1	Q12792	Twinfilin-1
U2AF1	Q01081	Splicing factor U2AF 35 kDa subunit
U2AF2	P26368	Splicing factor U2AF 65 kDa subunit
U520	O75643	U5 small nuclear ribonucleoprotein 200 kDa helicase
U5S1	Q15029	116 kDa U5 small nuclear ribonucleoprotein component
UAP1	Q16222	UDP-N-acetylhexosamine pyrophosphorylase
UAP56	Q13838	Spliceosome RNA helicase BAT1
UBA6	A0AVT1	Ubiquitin-like modifier-activating enzyme 6
UBF1	P17480	Nucleolar transcription factor 1
UBP10	Q14694	Ubiquitin carboxyl-terminal hydrolase 10
UBP2L	Q14157	Ubiquitin-associated protein 2-like
UFD1	Q92890	Ubiquitin fusion degradation protein 1 homolog
UGDH	O60701	UDP-glucose 6-dehydrogenase
USO1	O60763	General vesicular transport factor p115
USP9X	Q93008	Probable ubiquitin carboxyl-terminal hydrolase FAF-X
VIME	P08670	Vimentin
VIR	Q69YN4	Protein virilizer homolog
VPS29	Q9UBQ0	Vacuolar protein sorting-associated protein 29
VPS35	Q96QK1	Vacuolar protein sorting-associated protein 35
VPS53	Q5VIR6	Vacuolar protein sorting-associated protein 53 homolog
WDR1	O75083	WD repeat-containing protein 1
WDR5	P61964	WD repeat-containing protein 5
XPO2	P55060	Exportin-2
XPO5	Q9HAV4	Exportin-5
XRCC5	P13010	X-ray repair cross-complementing protein 5
XRCC6	P12956	X-ray repair cross-complementing protein 6
XRN2	Q9H0D6	5'-3' exoribonuclease 2
ZEB2	O60315	Zinc finger E-box-binding homeobox 2
ZN207	O43670	Zinc finger protein 207

Table S2. Evaluation of Spliceosomal Proteins in Complex with EWS-FLI1

Antibody used for WB	Antibody used for IP: FLI1 IP	PRPF8 IP	DDX5 IP
DDX5 ★	+	+	+
PRPF6 ★	+	+	+
hnRNP K ★	+	+	+
RHA ★	+	**0**	+
hnRNP U ★	+	+	+
CDC5L ★	+	+	+
DDX17 ★	+	**0**	+
SF3B3 ★	+	+	**0**
SF3B2 ★	**0**	+	+
SF3A2	+	+	+
PRPF8	+	+	**0**
SFPQ	+	+	+
SNRNP200	+	+	+
FLI1	+	+	+

Antibodies used for Co-IP are indicated on the top and the proteins tested by western blot antibodies are shown on the left. Experimentally validated binding partners of EWS-FLI1 are indicated by +, no co-IP indicated by 0. Commercially obtained recombinant purified proteins used for the ELISA experiments indicated by ★ , with those proteins directly binding to EWS-FLI1 shaded by a grey box.

Table S3A. Alternatively Spliced Genes Showing Various Events in EWS-FLI1 Reduction.

Event	Symbol	PSI Difference
SE	ABI1	-0.29
SE	ABI1	-0.32
SE	AK022898	-0.43
SE	AMD1	0.37
SE	ANK2	-0.26
SE	ANXA2	0.31
SE	ARFIP1	-0.33
SE	ATP13A3	-0.29
SE	B3GNTL1	-0.55
SE	BCAS4	-0.56
SE	BCLAF1	0.24
SE	BPTF	-0.27
SE	BPTF	-0.31
SE	BRD8	-0.32
SE	BRD8	-0.29
SE	C10orf118	0.21
SE	C10orf137	-0.63
SE	CAB39L	0.46
SE	CBWD1	-0.22
SE	CCDC144A	0.34
SE	CCDC88A	-0.27
SE	CD164	-0.22
SE	CLK1	0.33
SE	CLUL1	-0.57
SE	CNOT2	-0.24
SE	COL4A5	-0.36
SE	COQ5	-0.21
SE	CRYZ	0.21
SE	CUTC	0.41
SE	DCAF6	-0.43
SE	DCAF6	-0.37
SE	DEPDC1	0.23
SE	DEPDC1	0.2
SE	DIS3L2	-0.37
SE	DTYMK	-0.23
SE	DYRK4	-0.47
SE	EIF5	0.3
SE	EPB41	-0.58
SE	EPB41L2	-0.43
SE	EXOG	-0.49
SE	FAM126A	-0.41
SE	FAM126A	-0.25
SE	FAM126B	-0.32
SE	FAM126B	-0.24
SE	FAM192A	-0.26
SE	FAM192A	-0.36
SE	FAM60A	-0.22
SE	GPR126	-0.39
SE	GSTM1	0.32
SE	GUSB	0.55
SE	HBP1	0.43
SE	HM13	-0.2
SE	HMBOX1	-0.37
SE	HMGN1	-0.48
SE	HNRPDL	-0.35
SE	IFI44	0.23
SE	IFT46	-0.41
SE	IMMT	0.5
SE	ITGB1	0.38
SE	KIAA1731	0.46
SE	KIF23	-0.31
SE	KMT2E	0.45
SE	KRBOX4	0.27
SE	KRBOX4	0.25
SE	KTN1	0.31
SE	LAMP2	0.38
SE	LARP4	0.33
SE	LOC81691	0.47
SE	MAGOHB	-0.38
SE	MAGOHB	-0.32
SE	MCUR1	-0.63
SE	MDM1	-0.35
SE	MIS12	0.25
SE	MON2	-0.44
SE	MRPL30	-0.22
SE	MTMR2	0.43
SE	MYC	-0.2
SE	MYL6	-0.35
SE	NASP	-0.24
SE	NFYA	-0.59
SE	NQO2	-0.54
SE	NUMB	-0.21
SE	PAK1	-0.48
SE	PAPD4	0.28
SE	PDGFC	0.51
SE	PDPR	0.28
SE	PEX2	-0.3
SE	PFDN5	-0.3

SE	PFDN5	-0.35
SE	PHC3	-0.23
SE	PICALM	0.27
SE	PIGT	0.22
SE	PLOD2	-0.4
SE	PPFIBP1	-0.33
SE	PPP1R11	-0.3
SE	PRKDC	0.2
SE	PRMT2	-0.2
SE	PRMT2	-0.36
SE	PRPF39	-0.48
SE	PRPF39	-0.32
SE	RNPC3	-0.53
SE	RPAIN	-0.28
SE	RPL24	0.32
SE	RPS24	-0.45
SE	SAYSD1	0.37
SE	SBDSP1	-0.32
SE	SCAF11	0.22
SE	SEPT6	-0.58
SE	SEPT6	-0.44
SE	SLAIN2	-0.32
SE	SLC37A3	-0.37
SE	SLC38A9	-0.54
SE	SLIT2	-0.42
SE	SNED1	-0.48
SE	SON	-0.25
SE	SPAG9	-0.51
SE	SRSF11	-0.2
SE	SRSF7	-0.22
SE	SSFA2	-0.31
SE	STAG3L2	-0.29
SE	STAG3L4	-0.2
SE	SUSD5	0.44
SE	SYNE1	-0.58
SE	THTPA	0.4
SE	TIMM8B	0.23
SE	TMEM18	0.3
SE	TMEM209	-0.21
SE	TRA2B	-0.29
SE	TRPS1	0.4
SE	TTC9C	-0.2
SE	UAP1	-0.22
SE	UAP1	-0.23
SE	WDR35	0.31
SE	ZEB2	-0.2
SE	ZFP69B	-0.58

SE	ZFYVE20	0.44
SE	ZNF317	-0.53
SE	ZNF410	-0.23
SE	ZNF655	-0.31
RI	ABCC5	-0.33
RI	ABCF3	-0.35
RI	ANAPC5	-0.21
RI	AP1G2/AX747770	-0.23
RI	APEX1	-0.34
RI	APEX1	-0.41
RI	ARPC3	-0.22
RI	ATG16L1	-0.55
RI	BDH2	-0.33
RI	C17orf76-AS1	-0.33
RI	C3orf17	-0.32
RI	C7orf63	-0.46
RI	CCDC14	-0.52
RI	CCDC90B	-0.54
RI	CDCA7	-0.41
RI	CDK5RAP3	-0.52
RI	CDK5RAP3	-0.63
RI	CDK5RAP3	-0.34
RI	CDK5RAP3	-0.56
RI	CEP192	-0.29
RI	CIAO1	-0.38
RI	CLK1	-0.38
RI	CLK4	-0.28
RI	CLK4	-0.21
RI	CPNE1	-0.23
RI	CREB3L4	-0.38
RI	CSTF3	-0.3
RI	CTC1	-0.24
RI	CTNNB1	-0.2
RI	CTPS1	-0.56
RI	DDX47	-0.49
RI	DDX5	-0.2
RI	DHRS1	-0.23
RI	DYNC1I2	-0.43
RI	EFHC1	-0.33
RI	EIF2B5	-0.21
RI	ERCC3	-0.24
RI	ERCC3	-0.53
RI	FAM96B	-0.28
RI	FANCI	-0.41
RI	FLAD1	-0.42
RI	FN1	0.48
RI	FTH1	-0.57

RI	FTSJ1	-0.53
RI	GALT	-0.38
RI	GALT	-0.29
RI	GALT	-0.25
RI	GAPOA1BP /GPATCH4	-0.6
RI	GAS5	-0.37
RI	GPS2/NEURL4	-0.4
RI	GSS	-0.25
RI	GTF2H2	-0.31
RI	GTF2H4	-0.52
RI	HAX1	-0.22
RI	HCG18	-0.26
RI	HFE	-0.64
RI	HLTF	0.2
RI	HMGN2	-0.47
RI	HNRNPH1	-0.25
RI	HUS1	0.35
RI	IBTK	-0.39
RI	IDH3A	-0.22
RI	IFT80	-0.55
RI	ILK	-0.38
RI	IMP4	-0.69
RI	IP6K2	-0.4
RI	IP6K2	-0.39
RI	IP6K2	-0.37
RI	KIAA0141	-0.21
RI	LUC7L3	-0.44
RI	MARCH6	-0.75
RI	MARS	-0.26
RI	MARS	-0.26
RI	METTL17	-0.54
RI	MIR22HG	-0.23
RI	MMS22L	-0.28
RI	MRPL30/MITD1	-0.45
RI	MYL6B	-0.52
RI	NBPF10/RBM8A	-0.67
RI	NBPF10/RBM8A	-0.47
RI	NDUFAF7	-0.63
RI	NECAP1	-0.31
RI	NELFCD	-0.24
RI	NELFCD	-0.29
RI	NGDN	-0.44
RI	NIT2	-0.45
RI	NONO	-0.38
RI	NOP2	-0.3
RI	NR2C1	-0.41

RI	OSGEPL1	-0.2
RI	OXA1L	-0.28
RI	PDCD2	-0.26
RI	PHKG2	-0.39
RI	PNP	-0.21
RI	POLR1C	-0.22
RI	POLR2G	-0.22
RI	POLR2J4	0.47
RI	PQBP1	-0.32
RI	PRAME	-0.57
RI	PRMT2	0.2
RI	PRPF39	-0.56
RI	PSMA1	-0.33
RI	PSME2	-0.29
RI	PTGR2/ZNF410	-0.41
RI	QARS3	-0.53
RI	QKI	-0.2
RI	QKI	-0.27
RI	QKI	-0.26
RI	RAB3IP	-0.52
RI	RABGGTB	-0.33
RI	RBM3	-0.38
RI	RBM5	-0.51
RI	RBM6	-0.38
RI	RCHY1	-0.54
RI	RIOK1	-0.25
RI	RPL4	-0.22
RI	RPL7A	-0.25
RI	RPS21	-0.24
RI	SHISA5	0.22
RI	SLC25A3	-0.27
RI	SMARCC2	-0.27
RI	SNHG11	-0.44
RI	SNHG11	-0.41
RI	SNHG17	-0.47
RI	SOD2	0.31
RI	SRSF5	-0.5
RI	SRSF7	-0.31
RI	STAG3	-0.59
RI	SUPT7L	-0.36
RI	TCEB2	-0.26
RI	TIAL1	-0.31
RI	TIMM21	-0.24
RI	TMEM41B	0.28
RI	TMX2	-0.59
RI	TRMT13	-0.3
RI	TTC14	-0.24

RI	TTC8	-0.26
RI	U2AF1	-0.43
RI	UBXN4	-0.33
RI	VDAC2	-0.53
RI	WDR19	-0.27
RI	WDR6	-0.39
RI	WDR73/AL357213	-0.24
RI	XPOT	-0.48
RI	YBX3	-0.2
RI	ZNF10/ZNF268	-0.41
RI	ZNF226	-0.27
RI	ZNF232	-0.26
RI	ZSCAN26	-0.54
RI	ZWINT	-0.33
RI	ZWINT	-0.29
MXE	ABI1	0.23
MXE	AGPAT4	0.24
MXE	ANKRD10	-0.39
MXE	ANKRD10	-0.4
MXE	ANXA2	0.2
MXE	ARHGEF9	0.44
MXE	ARL13B	-0.47
MXE	BCS1L	0.4
MXE	BRE	-0.22
MXE	C20orf24	-0.48
MXE	CANX	-0.61
MXE	CD164	-0.29
MXE	DCAF6	-0.46
MXE	DPP8	0.42
MXE	GPD1L	0.38
MXE	H2AFY	0.44
MXE	HMGN1	-0.55
MXE	HMGN1	-0.31
MXE	HMGN1	-0.41
MXE	KIAA1191	0.25
MXE	LOC100132247	0.48
MXE	MYC/PVT1	-0.42
MXE	PGAP2	-0.47
MXE	PIGF	0.37
MXE	PRMT5	-0.22
MXE	PSMA1	-0.4
MXE	RFFL	0.53
MXE	SRP9	-0.28
MXE	STK36	-0.55
MXE	TATDN3	-0.43
MXE	TFPI	-0.36
A5SS	AURKB	-0.45

A5SS	BDH2	-0.34
A5SS	BORA	-0.62
A5SS	C12orf65	-0.22
A5SS	C12orf65	-0.4
A5SS	CHD9	-0.37
A5SS	CLIP4	0.59
A5SS	CLK4	-0.24
A5SS	CWC25	-0.63
A5SS	DNAJC16	-0.2
A5SS	GSTK1	-0.54
A5SS	IP6K2	-0.32
A5SS	ITFG2	-0.21
A5SS	KIF21A	-0.27
A5SS	LSM1	-0.22
A5SS	METAP1D	-0.39
A5SS	MRPL43	0.37
A5SS	PARK7	-0.6
A5SS	PARP2	0.33
A5SS	PNISR	-0.4
A5SS	POPDC3	-0.3
A5SS	PSMC3IP	-0.32
A5SS	RPAIN	-0.22
A5SS	SCNM1	-0.37
A5SS	SUPT7L	-0.26
A5SS	THTPA	0.36
A5SS	THTPA	0.37
A5SS	THTPA	0.37
A5SS	TIA1	-0.53
A5SS	TJP1	0.39
A5SS	YY1AP1	-0.57
A5SS	YY1AP1	-0.62
A5SS	ZSCAN26	-0.43
A3SS	ATP10D	0.2
A3SS	BOLA2	-0.34
A3SS	BX538249	-0.4
A3SS	FUS	-0.36
A3SS	GIT2	0.59
A3SS	INTU	-0.22
A3SS	ISCU	-0.63
A3SS	ITGB1BP1	-0.34
A3SS	KIAA0430	0.33
A3SS	LDHA	0.41
A3SS	LINC00667	-0.84
A3SS	LUC7L	-0.57
A3SS	METTL17	-0.22
A3SS	MFF	-0.58
A3SS	NCOA7	0.31

A3SS	ORMDL1/PMS1	-0.32
A3SS	PDE4DIP	0.43
A3SS	PFDN5	-0.46
A3SS	POP5	0.33
A3SS	PPP6R3	-0.54
A3SS	QKI	-0.34
A3SS	RNF216	-0.23
A3SS	SREK1	-0.43
A3SS	SRSF5	-0.47
A3SS	STAG3L4	-0.22
A3SS	STRADB	0.54
A3SS	SUPT20H	-0.24
A3SS	SUPT20H	-0.43
A3SS	TMEM39A	0.47
A3SS	TUG1	-0.2
A3SS	WSB1	-0.5
A3SS	ZNF106	-0.31

Both EWS-FLI1 reduction and YK-4-279 treatment, with common alternatively spliced genes shaded in blue.

Table S3B. Alternatively Spliced Genes Showing Various Events in YK-4-279 treatment.

Event	Symbol	PSI Difference
SE	AK311356	0.49
SE	AK311578	0.53
SE	AK311578	-0.39
SE	AKR1A1	-0.33
SE	ALDH3A2	0.23
SE	ANAPC16	0.28
SE	ANXA2	0.53
SE	ASCC1	-0.49
SE	ASCC1	-0.52
SE	ATXN2	0.58
SE	BBX	-0.5
SE	C10orf137	-0.47
SE	C14orf159	0.35
SE	C14orf159	0.33
SE	CCDC169	-0.45
SE	CD46	-0.33
SE	CDCA7L	0.2
SE	CNOT4	-0.3
SE	EIF3M	-0.62
SE	EIF3M	-0.24
SE	EIF3M	-0.57
SE	EIF4A2	-0.2
SE	EXOSC3	0.24
SE	FAM221A	-0.72
SE	FAM64A	0.37
SE	FLJ31306	-0.38
SE	GPR64	-0.29
SE	HNRNPA1L2	-0.42
SE	HNRNPR	0.21
SE	HNRNPR	0.21
SE	HPS5	-0.34
SE	JAKMIP2	0.27
SE	KMT2E	0.36
SE	LTA4H	0.25
SE	METTL22	0.32
SE	MLH1	0.25
SE	MTFP1	0.34
SE	MTFP1	0.35
SE	MTFP1	0.35
SE	MTUS1	-0.42
SE	NEK1	-0.45
SE	NUP62	-0.32
SE	OARD1	-0.24
SE	P4HA1	0.36
SE	PCM1	-0.31
SE	PIGT	0.24
SE	PIGT	0.37
SE	PIGT	0.55
SE	PIGT	0.3
SE	PPFIBP1	-0.39
SE	PRPF39	-0.29
SE	R3HCC1L	-0.2
SE	RBMS3	0.51
SE	RNF19A	-0.3
SE	RNF19A	-0.27
SE	RPL17	0.22
SE	SCAF11	0.21
SE	SETD9	0.24
SE	SETD9	0.23
SE	SLC29A3	0.41
SE	THADA	-0.33
SE	TMEM18	0.31
SE	TNC	0.41
SE	TPP2	-0.27
SE	TRIM37	0.32
SE	TRPS1	0.4
SE	TTC17	-0.23
SE	UBAP2L	-0.32
SE	UTS2B	0.5
SE	VPS29	0.32
SE	YWHAB	-0.52
SE	ZFP69B	-0.31
SE	ZNF138	-0.31
SE	ZNF655	-0.51
RI	CLK1	0.24
RI	DCTN1	-0.29
RI	ELP5	0.21
RI	FN1	0.4
RI	IFT80	-0.51
RI	KIAA0141	-0.21
RI	NBPF10/PIAS3	-0.22
RI	POLR2J4	0.51
RI	PRPF39	0.47
RI	RECQL	-0.21
RI	RPL28	0.35
RI	RPS9	0.26
RI	RPS9	0.38
RI	SYNE1	-0.31

RI	SYNGR1/TAB1	-0.33
RI	TMEM234	0.28
RI	VAMP4	-0.25
MXE	ANXA2	0.43
MXE	BOLA2/HIRIP3	0.29
MXE	DPP8	0.64
MXE	EMC4	0.21
MXE	EYA4	0.35
MXE	GTF2H1	0.41
MXE	GTF2H1	0.38
MXE	MCTP1	-0.61
MXE	NDUFS1	0.35
MXE	NDUFS1	0.23
MXE	NELFA	-0.57
MXE	NUBP1/TVP23A	-0.31
MXE	POLK	-0.2
MXE	PRKAG1	-0.62
MXE	RAP1GDS1	0.2
MXE	SETD9	0.38
MXE	SETD9	0.35
MXE	ZNF561	0.55
A5SS	ANKRD49	0.28
A5SS	ANKRD49	0.38
A5SS	CSNK1A1	0.31
A5SS	CUL4B	-0.51
A5SS	DNAJC16	-0.37
A5SS	EIF1AD	-0.32
A5SS	ENPP3	-0.45
A5SS	FIGNL1	0.36
A5SS	FIGNL1	0.34
A5SS	GOLGB1	-0.57
A5SS	MRPL51	0.33
A5SS	ODF2	0.42
A5SS	PNISR	0.3
A5SS	PTCD2	-0.38
A5SS	PUM2	-0.25
A3SS	APTX	-0.4
A3SS	ATP10D	0.32
A3SS	CD320	-0.59
A3SS	CEP85	0.29
A3SS	DNAJC9	0.26
A3SS	E2F5	-0.45
A3SS	FAM213A	-0.21
A3SS	HELZ	-0.36
A3SS	IMMT	-0.52
A3SS	PAN2	-0.23
A3SS	ZC3H14	0.26

Both EWS-FLI1 reduction and YK-4-279 treatment, with common alternatively spliced genes shaded in blue.